AWARD NUMBER: W81XWH-13-1-0349

TITLE: N-Terminal Tau Fragments as Biomarkers for Alzhelmer’s Disease and Neurotrauma

PRINCIPAL INVESTIGATOR: Garth F. Hall Ph.D.

CONTRACTING ORGANIZATION: University of Massachusetts Lowell
Lowell, MA 01854

REPORT DATE: December 2017

TYPE OF REPORT: Final

PREPARED FOR: U.S. Army Medical Research and Materiel Command
Fort Detrick, Maryland 21702-5012

REPORT DOCUMENTATION PAGE

Form Approved
OMB No. 0704-0188

1. REPORT DATE December 2017

2. REPORT TYPE Final

3. DATES COVERED 30Sept2013 - 29Sept2017

4. TITLE AND SUBTITLE
N-Terminal Tau Fragments as Biomarkers for Alzhelmer's Disease and Neurotrauma

5a. CONTRACT NUMBER

5b. GRANT NUMBER W81XWH-13-1-0349

5c. PROGRAM ELEMENT NUMBER

6. AUTHOR(S)
Dr. Garth Hall

E-Mail: dabize@gmail.com

5d. PROJECT NUMBER

5e. TASK NUMBER

5f. WORK UNIT NUMBER

7. PERFORMING ORGANIZATION NAME(S) AND ADDRESS(ES)

University of Massachusetts Lowell
Lowell, MA 01854

8. PERFORMING ORGANIZATION REPORT NUMBER

9. SPONSORING / MONITORING AGENCY NAME(S) AND ADDRESS(ES)

U.S. Army Medical Research and Materiel Command
Fort Detrick, Maryland 21702-5012

10. SPONSOR/MONITOR'S ACRONYM(S)

11. SPONSOR/MONITOR'S REPORT NUMBER(S)

12. DISTRIBUTION / AVAILABILITY STATEMENT

Approved for Public Release; Distribution Unlimited

13. SUPPLEMENTARY NOTES

14. ABSTRACT
The goal of this project is project was to increase our understanding of the underlying causes of both CTE and AD and by so doing, improve our ability to diagnose the presence and severity of these conditions in a timely manner. Our approach was based on observations that tau isoforms lacking exons 2-3 in the tau N terminal domain (E2- tau) are secreted more readily than isoforms that contain one or both of them (E2+ tau) in cell culture (Kim et. al. 2010) and that secreted microvesicles (exosomes) containing tau and other proteins are identifiable in the cerebrospinal fluid (CSF) of patients, in the early stages of AD (Saman et al 2012). The Aims of the project were to 1) characterize the cellular distribution of E2+ and E2- tau isoforms in fixed brain tissue from early AD and CTE patients, to quantify their presence in CSF and brain homogenate exosomal fractions and to identify proteins associated with tau (and particularly E2- and E2+ tau) in these fractions in the context of AD/CTE cytopathogenesis. The second Aim of this project was to directly test the effects of overexpressing E2- and E2+ tau isoforms on tau distribution, secretion and the recruitment of other proteins to exosomes in neuronal cell lines (by mass spectrometry).

15. SUBJECT TERMS

Nothing listed

16. SECURITY CLASSIFICATION OF:			17. LIMITATION OF ABSTRACT	18. NUMBER OF PAGES	19a. NAME OF RESPONSIBLE PERSON USAMRMC
a. REPORT	b. ABSTRACT	c. THIS PAGE			19b. TELEPHONE NUMBER *(include area code)*
Unclassified	Unclassified	Unclassified	UU	33	

Table of Contents

1 Introduction

The goal of this project is project was to increase our understanding of the underlying causes of both CTE and AD and by so doing, improve our ability to diagnose the presence and severity of these conditions in a timely manner. Our approach was based on observations that tau isoforms lacking exons 2-3 in the tau N terminal domain (E2- tau) are secreted more readily than isoforms that contain one or both of them (E2+ tau) in cell culture (Kim et. al. 2010) and that secreted microvesicles (exosomes) containing tau and other proteins are identifiable in the cerebrospinal fluid (CSF) of patients, in the early stages of AD (Saman et al 2012). The Aims of the project were to 1) characterize the cellular distribution of E2+ and E2- tau isoforms in fixed brain tissue from early AD and CTE patients, to quantify their presence in CSF and brain homogenate exosomal fractions and to identify proteins associated with tau (and particularly E2- and E2+ tau) in these fractions in the context of AD/CTE cytopathogenesis. The second Aim of this project was to directly test the effects of overexpressing E2- and E2+ tau isoforms on tau distribution, secretion and the recruitment of other proteins to exosomes in neuronal cell lines (by mass spectrometry).

This constitutes the final technical report of the results of W81XWH-13-1-3949. Overall, I believe we have met the stated Specific Aims of the project successfully, although this includes both overperforming (Aims 1A and especially 1B) and underperforming (Aim 2A and especially 2B) returns from individual Aims. Satisfactory completion of the project (and thus the submission of this report) was greatly delayed by our decision to complete the AD/CTE comparative characterization experiments, which became possible (i.e. sufficient samples collected) only toward the end of the original grant period, but was obviously of the most critical importance to the overall significance and in particular, the military relevance of the project. Completion of this work was delayed beyond the end of the NCE by a) the sheer volume of IHC runs, the subsquent image montaging sessions at the Jamaica Plain VA and finally the analysis summarized in this Report, most of which had to be performed personally by the PI. These delays were further exacerbated by the necessity of finishing the project on a collaborative rather than a fee for service basis, owing to the lack of personnel funds. We hope that our results compensate the administrative staff at PRARP for the inconveniences caused by the delayed subimssion of this Final Technical Report.

In this final report, we describe the completion of Aim 1, where we have characterized N terminal isoform (E2-) tau-specific cellular and extracellular lesions that form in the dentate gyrus and CA1 of the hippocampus during the course of AD.We add to earlier descriptions of these lesions as follows: Our discovery and comparative characterization of this novel lesion type in AD and CTE constitutes the major result from this investigation and is likely to have a significant impact on our understanding of the pathogenesis of AD, CTE and the mechanisms that connect these conditions. Other aspects of Aim 1 (the completion of manuscripts for publication) have been delayed by the necessity of reanalysis in light of new findings in the literature (that suggest a link between CSF tau isoforms and miRNA control of gene expression patterns) are nearing completion. The nature of these reanalyses and the conclusions drawn from them are summarized. We met major technical challenges in conducting the cellular studies proposed for Aim 2 and were forced to reduce the scope of the remaining cellular localization studies, the results of which are described in this report. The bulk of the NCE funds were spent on IHC supplies in support of the comparative IHC studies of the E2- tau lesions in AD and CTE. This work was done in collaboration with Drs. Ann McKee, Dharmendra Goswami and Dr. Russ Huber and thus did not require personnel funds from this grant. All funds remaining in the grant at the end of the original funding period were spent as previously reported before the end of the NCE (9-30-2016).

2 Keywords

Tau isoforms
Alzheimer's Disease pathogenesis
AD links to CTE
Alzheimer's Disease CSF biomarkers
Bioinformatic analysis
Exosome
Extracellular microvesicle
Senile plaque
Hippocampus
MicroRNA

3 Overall Project Summary

Aim 1: Sensitivity and specificity of the N-Terminal Tau fragment as a biomarker

1A: Proteome analysis of CSF & brain homogenates

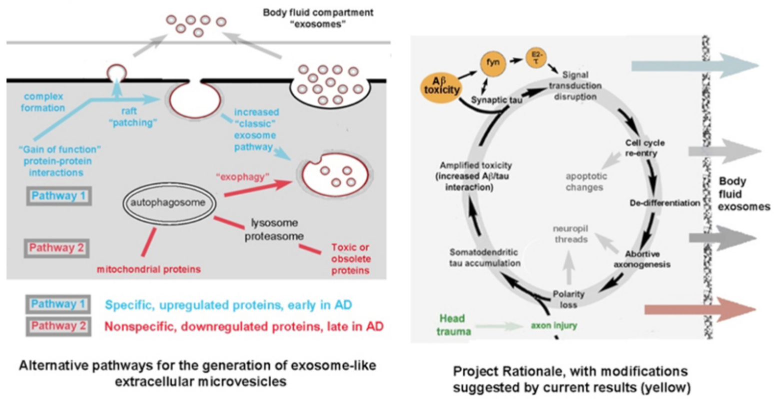

Figure 1: Left Panel: Two discrete mechanisms of up and downregulated proteins to exosomes (Bhatia & Hall, 2013). Upregulated proteins not normally present in exosomes but that are associated with protein and ribonucleoprotein complexes can be recruited to exosomes in interneuronal viral transfer and cancer (Pathway 1). There is also a well established "garbage can" pathway (Pathway 2) by which downregulated proteins in autophagosomes and/or lysosomes can be removed from the cell via "exophagy" (Abrahamsen & Stenmark 2011) . Right: Summary of the hypothesis informing this proposal (see attached MS draft). The onset of tauopathy causes gain of function changes associated with Ab accumulation that are mediated by tau-induced disruptions leading to cell cycle re-entry. These are reflected as Pathway 1 mediated diversion to the CSF exosomal proteome and include a) abnormal local interactions of postsynaptic tau with signaling pathways associated with nonsynaptic functions such as cell cycle control that may activate or increase cellular utilization of such pathways, resulting in their upregulation. This accounts for CCRE-associated changes in early AD and may indirectly cause the downregulation of genes that express neuron-specific proteins. This in turn causes de-differentiation and consequent downregulation and dumping of neuron-specific proteins via "exophagy" (Pathway 2), leading to axon damage, the failure of axonal localization of tau and increased tau diversion to sensitive loci in the dendrites.

1A Summary from previous reports We have completed the work reported previously on the AD CSF and hippocampal homogenate exosomal proteomes to include all of the 14 CSF samples from all Braak stages of AD (3 stages 3, 5 Stage 4, 4 Stage 5 and 2 Stage 6 cases) that we had adequate volumes of for mass spec proteome analysis and 10 hippocampal homogenate fractions of AD cases (1 Stage 3, 3 Stage 4, 2 Stage 5 and 4 Stage 6). We have analyzed both CSF and HC samples from 6 AD patients. CSF and HC samples from 10 VaD and MID (ischemic

dementia) served as controls. The previously reported analysis is summarized in Figures 2 and 3, To summarize the key findings briefly:

1) **Remarkably high ratio of proteins known to be upregulated in the 5 Braak Stage 4 CSF samples. This was accentuated in multipatient proteomes and was absent from Stage 4 HC samples, including those cases where the CSF and HC samples were from the same patient.**
2) **Recruitment pathways for both the upregulated in AD and downregulated in AD proteins identified in CSF proteomes have been identified in the literature, and are consistent with GO term functions known to be affected in AD (Figures 1 and 2).**
3) **The Stage 4 CSF samples with the highest up in AD/Down in AD ratios had significantly higher than average E2- ELISA scores relative to other AD stages, a feature that was most significant among those proteins that had been identified in multiple patients (Figure 3).**
4) **Multipatient proteins that are upregulated in AD were primarily direct or strong indirect interactors with tau or APP, suggesting a specific, gain-of toxic function relationship with AD pathogenesis, whereas proteins downregulated in AD tended to be unique to individual patients. "Down in AD" proteins were also more common in samples from established AD (Stages 5-6) and were much less specific to AD.**

1A Summary of new data obtained and analyses performed during the NCE While our earlier analysis identified both elevated proportions of E2- tau species and AD-specific upregulation of non-tau proteins in CSF exosomes, it yielded few hints as to how these features are or might be mechanistically linked. Since the elucidation of this relationship was an overriding goal of the project, we undertook a survey of possibly relevant recent findings in the literature while preparing this material for publication during the NCE. We found that many of the most interesting proteins in the Stage 4 CSF proteome (i.e. those that interact with tau/APP, are upregulated in early/moderate AD, and were identified in multiple samples) are also targets of microRNAs that are strongly expressed in the CNS, have been identified in exosomes or exosome-like extracellular microvesicles (EMVs) and are themselves downregulated in AD (Lau et. al. 2013). We also found that tauopathy-associated dysregulation of tau splicing (and thus tau isoform ratios) has been linked to miRNA downregulation in early AD (Smith et. al. 2011). Since such miRNAs might provide a link between high E2- ratios and AD-associated upregulation in CSF tau, we devoted significant effort to revising our MS to take account of these findings and identify (if possible) likely candidate miRNAs during the NCE. We also performed a reanalysis of multisample protein proteomes (with hippocampal exosome fractions added) to increase its sensitivity. This was possible because the relatively low overlap between hippocampal homogenate and CSF EMV30-200 proteomes indicated clearly that a protein occurring in both HC and CSF samples, even from a single patient, was very unlikely unlikely to be a random "hitchhiker". As a consequence of this reanalysis, we identified a "fingerprint" of 47 tau/Aβ interacting proteins (Figure 7) that largely account for the upregulated GO functions, which are generally thought to be gain-of-function toxic consequences of tau/Aβ interaction in early AD (see Figure 1). The results of these additional analyses are summarized in Figures 4-8 and in the following bullet points:

- **Multisample CSF/HC EMV30-200 proteome analysis based on physical interaction with tau and/or Aβ in the String database shows that a substantial proportion of early AD, but not established AD or VaD/MID EMV30-200 proteins, may have been recruited to EMVs as a gain-of function consequence of tau/Aβ interaction (Figure 4).**

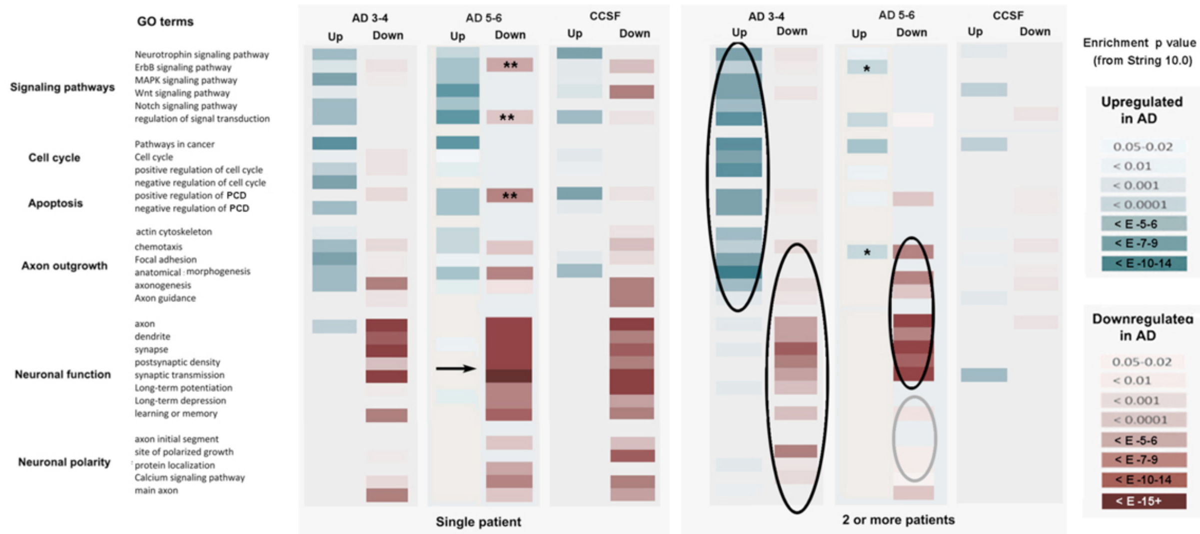

Figure 2: GO term analysis of AD-specific effects on the multipatient proteome Heat map showing the enrichment of uniquely occurring proteins (left) and multipatient proteins (right) in the AD and CCSF exosomal proteomes for changes in AD-relevant cellular functions (Figure 1). Enrichment is given as the p value returned by String for the enrichment of GO term members in each proteome relative to background. The intensity of upregulated (blue) and downregulated (red) according to the key at the bottom of the figure. GO term enrichment among uniquely occurring proteins from early (AD 3-4) and established (AD 5-6) shows the pattern predicted by our hypothesis (see text), but also resembles the MID/VaD (CCSF) controls, especially among downregulated functions. These points of resemblance disappear when proteins that appear only once in either the control or AD datasets are excluded (right), leaving a strong AD-specific pattern of enrichment for upregulated signal transduction, cell cycle and development terms and downregulated neuronal structures and functions, including markers of neuronal polarity. The addition of 2460 proteins identified in Stage 5 and Stage 6 shows a similar but not identical pattern to that seen with Stages 3-4. Some of these differences (i.e. the stronger representation of downregulated neuronal genes that were not present in multiple patients - see arrow) are readily explained by the involvement of much larger areas of the brain in Stages 5-6 over Stages 3-4. However, the Stage 5-6 "multiple patient" proteome does not retain the broad swath of upregulated GO terms seen with the Stage 3-4 proteome; only a few are enriched relative to both Stage 3-4 AD and controls (single asterisks). Also, there is a stronger representation of downregulated neuronal terms than was seen in Stage 3-4 AD (black oval), but this did not include synaptic plasticity and neuronal polarity.

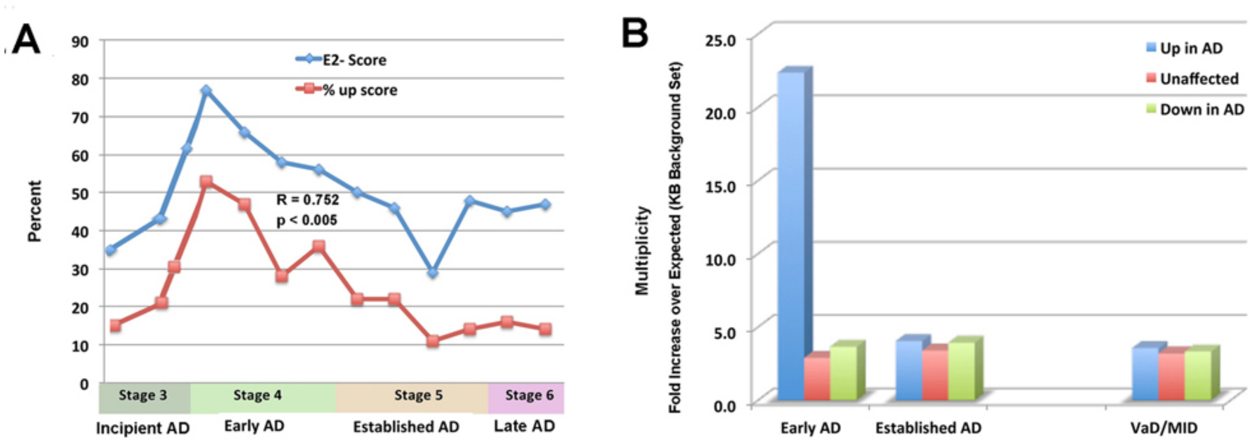

Figure 3 Significant correlations exist between Braak stage, E2- ELISA score, upregulation in AD and interactions between tau and Abeta These emerge from a bioinformatic comparison of CSF proteomes **Panel A:** E2-/E2+ ELISA ratios (shown as percentE2- scores) of CSF exosome fractions taken from early AD (Braak stage 4) patients and established AD (Braak stage 5-6) are plotted versus the ratio of upregulated/downregulated in AD proteins (x axis). This plot shows that both the proportion of upregulated gene products in CSF exosomes and the E2-/E2+ ELISA ratio in whole CSF show a peak at Braak Stage 4. The significant correlation between upregulation in AD and E2- score was verified by regression analysis), and that of the link between upregulation in AD and Braak stage is shown in **Panel B**, which shows a highly significant peak in early (Stage 4 $p << 0.00001$ vs either Stage 5-6) for "multiple patient" proteins. Multiplicity is shown as the fold increase in actual multipatient proteins over the number expected for the same proteome sizes if the degree of interproteome overlap were random.

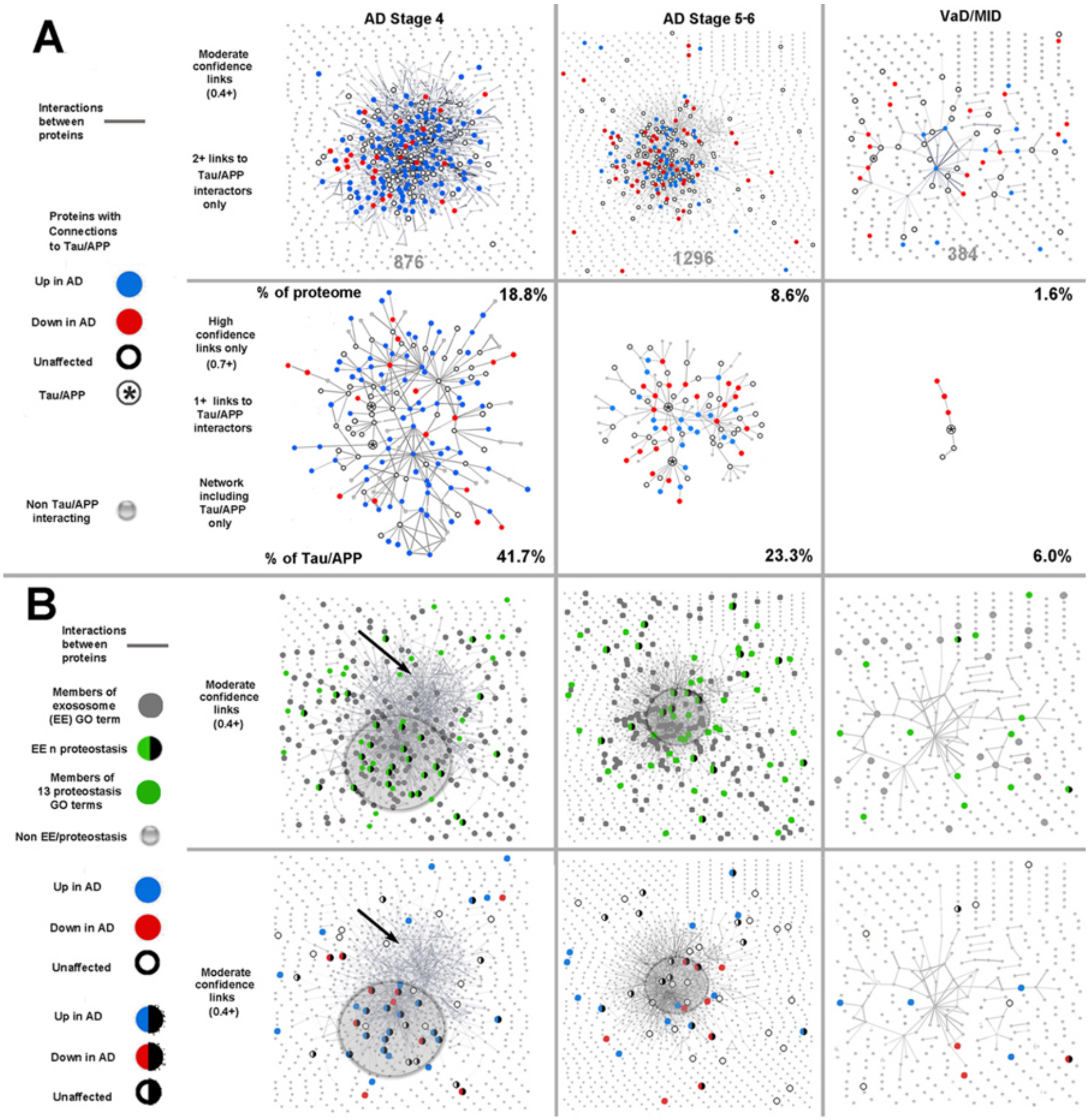

Figure 4 **Gain of function changes in the early AD CSF EMV proteome** Connectivity analysis of multiple set proteins from combined brain/CSF proteomes (including EE members) shows distinctive features of intraproteome interactions present in early (Braak stage 4) AD samples that distinguish them from established AD (Braak Stage 5) and VaD/MID proteomes. **Panel A** shows a high degree of both overall connectivity within the sample proteome and connectivity with tau/Aβ in early AD; this is significantly reduced in later stage AD and nearly absent in MID/VaD controls. This high connectivity in Stage 4 AD is mediated primarily by proteins upregiulated in AD (blue icons) and accounts for most of the intraproteome connectivity seen at the "moderate" (0.4 – top images) and high (0.7 – bottom images) threshold settings (Franceschini et. al. 2013). This can be seen more directly in the bottom row of Panel A, where intraproteome interactions "recruit" a significant proportion of the tau/Aβ interactors present to a common network that includes both APP and MAPT. A higher connectivity threshold (0.7 instead of 0.4), lower tau/ Ab threshold (1+ link instead of 2+ links) were used here and disconnected icons were omitted from this illustration for the sake of clarity. **Panel B:** An additional factor responsible for high relative interprotome connectivity of the early AD sample is the enrichment of highly connected proteins that are both members exosome GO term (extracellular exosomes or EE) and involved in proteostasis regulation (13 GO terms related to autophagy, lysosomal and proteosomal function – shown as hatched icons). EE members that were not proteostasis related and proteostasis related proteins that are not in the EE CO term are shown as gray and green icons, respectively. Unlike Tau/Aβ interaction, the significantly increased representation of EE and proteostasis proteins in Braak 4 AD relative to the others (and to the reference KB set) is not correlated to overall intraproteomal connectivity. Rather, we see a localized enrichment of proteins that are both EE and proteostasis linked in part of the highly connected region of the String diagram at Stage 4 (circle, left) and a relative depletion of such proteins in the remainder of the highly connected portion of the proteome (arrow, left). Note that this feature is no longer present in Stage 5-6 AD (circle/arrow, center). This pattern suggests that the early upregulation of EE members in AD (Figure 3A) is linked to an AD-specific but transient change in proteostasis regulation in early AD.

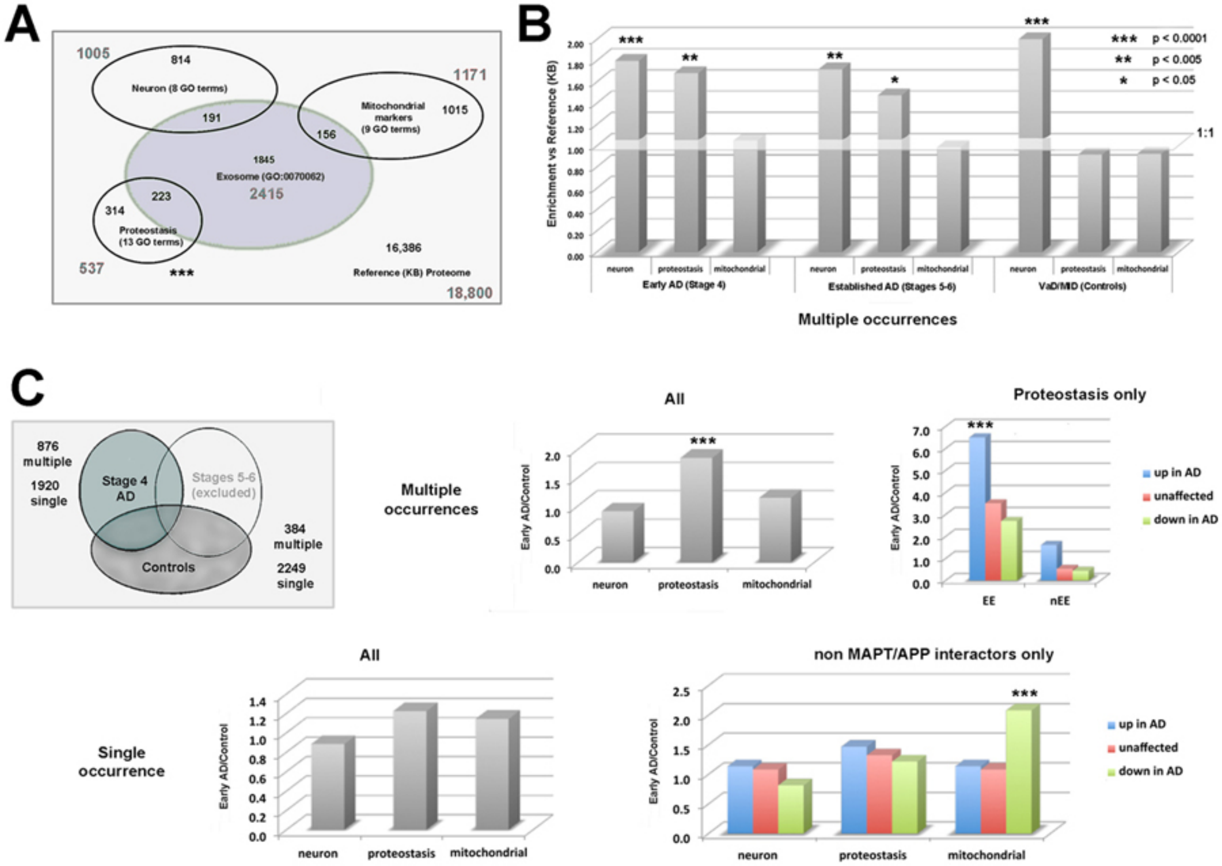

Figure 5 Recruitment of proteostasis regulation and autophagosome cargo proteins to CSF exosome-like microvesicles (EMV30-200) **Panel A:** Union of proteostasis, neuronal and mitochondrial composite sets with component GO terms are shown and the number of members of each in the reference set (KB). The degree of overlap of each of these composite sets with the exosome GO term (extracellular exosome - EE) are also shown. Note that the proteostasis set is significantly more enriched in EE members than the others . **Panel B:** Enrichment pattern of protein categories shown in A in stage 4 (early AD) Stage 5-6 (established AD) and ischemia control (VaD/MID) multisample CSF EMV30-200 proteomes. Proteins involved in macromolecular turnover mechanisms (proteostasis), but not autophagosome/lysosome cargo (mitochondrial markers) are enriched in early AD ($p < 0.001$, Fisher's Exact Test) but not ischemia dementia controls. The enrichment of neuronal GO term members in all samples relative to the reference set (marked by the translucent panel) may reflect contamination of EMV samples with apoptotic vesicles, which are typically much larger than 200 nm diameter, but have a broad size range range. **Panel C:** Enrichment of multisample (top) and single occurrence (bottom) proteins in the early AD samples relative to VaD/MID controls are shown (graphs, gray bars). Proteome sizes are shown in the Venn diagram at left. A breakdown of specific subproteomes by expression in AD category (up unaffected, down) is shown at right. The specific enrichment in upregulated proteostasis markers in Stage 4 AD via Pathway 1 is correlated with the enrichment of EMV30-200 proteomes with non APP/MAPT interacting mitochondrial markers (autophagy cargo) via Pathway 2.

Figure 6 Verification of AD associated changes in gene expression used in this project (Saman 2014) versus a recent "consensus" study of up/downregulated genes (Talwar, 2016). We found a category-specific rate of agreement of over 70% between proteins in both lists (Panel A). There was also a highly significant and category-specific enrichment of proteins cited in Talwar 2016 in the multisample early AD proteome members. This was most prominent among upregulated members, but was more significant among the default "unaffected" category due to proteome size (Panel B).

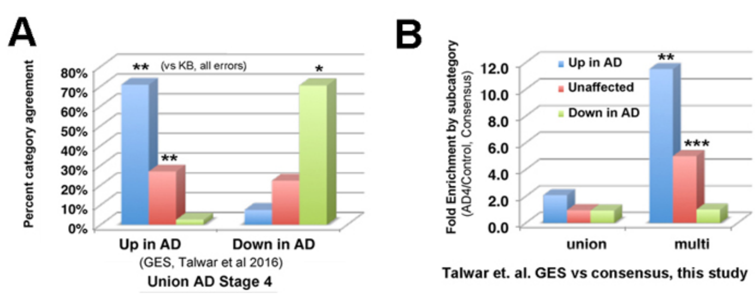

- **Multisample, (CSFor HC) EMV30-200 proteins that are upregulated in AD and associated with proteostasis mechanisms were strong interactors with tau or APP, whereas autophagosome cargo (exophagy) markers were downregulated in AD, were non-tau/Aβ interactors, suggesting recruitment by Pathways 1 and 2 (Figure 1) respectively (Figure 4, bottom panel, Figure 5).**
- **Reanalysis of key members of upregulated and downregulated genes in AD of key subproteomes to validate the published (and previously reported) reference list (Saman et. al. 2014, First Quarterly Report for this project), found verification of most of them in recent microarray-based analysis of dysregulated gene products (Talwar et. al. 2016 - Figure 6).**
- **A 47 member "fingerprint" of multisample, tau/Aβ-interacting proteins that are upregulated in AD and not members of the exosome (EE) GO term account for most of the GO-term enrichment pattern seen in the larger (876 member) early AD multisample proteome (Figure 7)**
- **Fingerprint members and their functional interactors are significantly enriched in targets of a tau-interacting miRNA (mi-R132-3p) downregulated in early AD (Figure 8)**

B) Immunohistochemistry study of AD and CTE paraffin-embedded brain sections

1B Summary of previously reported progress IHC analyses of AD and CTE derived sections of fixed brain tissue using E2- and E2+ isoform-specific mAbs undertaked in this project have yielded significant additions to our knowledge of AD and CTE pathogenesis. This Final Report has been delayed primarily because of difficulties in acquiring hippocampal (HC) tissue from late stage CTE (Stage 3-4 – McKee et. al. 2013) cases that could be processed in parallel with new incipient (Stage 2) and established (Stage 5) AD hippocampal samples. We required enough CTE HC samples to make credible comparisons between propagated tau lesions in CTE and AD.

Sample acquisition summary The overall goal of the immunohistochemical arm of Aim 1 has been to compare the development of tau lesions in AD with those of CTE as comprehensively as possible so as to identify common mechanistic features underlying the intercellular propagation of neurofibrillary lesions in human patients. We have therefore focused on the hippocampus, since it is a CNS structure to which neurofibrillary lesions spread in both CTE and AD, but is not the site of lesion initiation in either AD or CTE. Over the course of this project, we have acquired and processed a total of 53 CNS tissue samples, of which 29 (17 AD and 12 CTE) were from clinically diagnosed cases that included lesion staged hippocampal tissue. Another 18 samples were from clinically diagnosed cases (6 AD and 12 CTE) in which neurofibrillary lesions had not yet reached the hippocampus, and an additional 6 samples were from prodromal AD like dementia (2), acute TBI (2), and from "control" cases without a history of dementia (2).

Immunolabeling We have immunostained10 micron sections with from largely hippocampal tissue blocks using E2- and E2+ isoform specific tau mAbs (9A1 and DC39). Additional targets for immunolabeling include MAP2, Abeta, synaptic terminal markers (bassoon) and various phosphorylated (pY18, pS202-205) and non-phosphorylated epitopes (residues 159 and 210) on tau. We have also used the mAb Iba1 (a marker for activated microglia) for recent correlative work directed at assessing common and distinctive features of propagated E2-/E2+ tau lesions between AD and CTE (reported below). The results of manually photomontaged sections and the reconstruction of single images from adjacent sections was previously reported and is summarized in Figure 9. Most of the Aim 1 IHC based findings in earlier quarterly and yearly reports for this project describe the development of hippocampal lesions in the dentate gyrus (DG) and CA1 in the pathogenesis of AD. These sites were chosen because they are early targets of neurodegeneration in

AD and are postsynaptic targets of the perforant pathway (PP) projecting from the entorhinal cortex (EC) to the HC. This work has resulted in the identification of a novel lesion type that reflects the postsynaptic deposition of tau species that lack the E2/3 alternatively spliced region in the N terminal domain. We summarize previously reported results with the E2- and E2+ mAbs (9A1 and DC39) in isocortex of AD and CTE cases reported earlier and have extended them regions of the hippocampus (HC) that are affected in the earliest stages of AD (DG, CA1) and as secondary loci for lesions spreading in CTE (CA1). The main lesion that we have observed in AD HC loci consists of localized interstitial E2- tau-specific deposits associated with swollen E2- positive presynaptic terminals. These are present in both the DG and in CA1 pyramidal dendritic fields, but are more readily characterized in the molecular layers (OML and IML) of the DG, where they are surrounded by the dendrites of granule cells (GCs) which typically do not develop NFTs in AD. We have called these flocculent tau lesions (FTLs). FTLs may be associated with A beta plaques in various stages of development and are associated with localized toxicity as shown by the loss of MAP-2 immunolabel from dendrites of nearby GCs (dentate) and pyramidal neurons (CA1/subiculum). Although we have identified E2- positive FTLs in the DG in the absence of Abeta immunolabel in MAP2/Abeta double-labeled sections, it remains possible that cellular changes underlying FTL generation are a consequence of A beta-mediated toxicity (rather than a possible contributor to SP formation), depending on the sensitivity of the A beta and E2- specific mAbs (i.e. the presence of sub-IHC threshold A beta deposits).

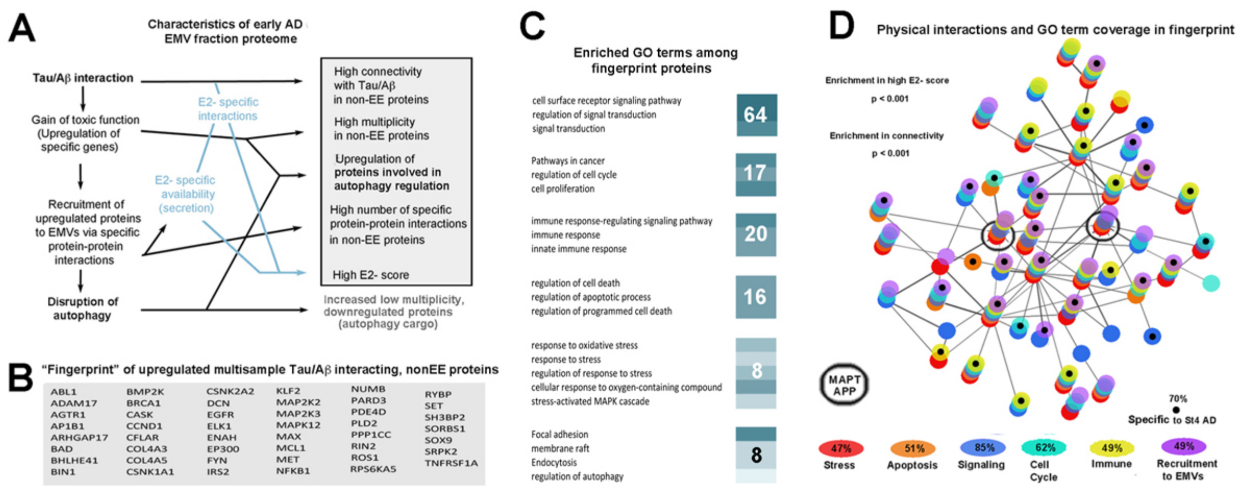

Figure 7: The CSF EMV fraction proteome from early AD CSF and hippocampal homogenate samples yields a functionally coherent "fingerprint" consistent with AD-related miRNA dysregulation and toxic interactions between tau and Aβ **Panel A s**ummarizes the observed features of the early AD (Braak Stage 4) proteome and their putative links to two established features of AD neuropathogenesis – tau/Aβ toxic interaction and the disruption of normal autophagy. Hypothesized links relevant to E2- tau enrichment are shown in blue. **Panel B** lists 47 proteins that are upregulated in AD, were identified in multiple CSF and HC EMV30-200 samples and have direct or strong indirect physical interactions with tau/Aβ. Panel C: Representative GO terms that are significantly enriched for the 47 protein fingerprint that describe cellular strunctures and functions affected in early AD (Figure 1). The total number of enriched terms for each category are also shown (white overlay). Panel D: Connectivity map of the 47 "fingerprint terms plus tau (MAPT) and APP (black circles). Note that the fingerprint members with the highest degree of connectivity to tau and Aβ also have the most relevance to early AD GO term categories.

Our approach was to use the DG to characterize FTLs in isolation from NFTs/pretangles, and then to compare the 2 lesion types and their development in CA1. Additional reported results are summarized as follows:

- **Slight increases in the size and elaborations of microglia near DG FTLs in AD, suggesting roles for pro-inflammatory changes and (possibly) A beta toxicity in FTL formation.**

- **In intracellular NFT-like tau lesions, E2- tau is largely colocalized with but somewhat more distally distributed than E2+ tau in CA1/subicular pyramidal neurons.**
- **E2- tau is distributed in a less cytoskeletal pattern than is E2+ tau in CA1 and other HC pyramidal somata and dendrites, and is more frequently present on punctate bodies in the neuropil that appear to be synaptic terminals. Significant MAP-2 loss in CA1 pyramidal cells was seen in conjunction with 1) small FTLs consisting of swollen E2- positive PSTs surrounding single pyramidal cell somata, usually without Abeta deposits and 2) larger FTLs that are often associated with SP-like A beta deposits.**
- **The prominent reduction of somatodendritic MAP2 immunolabel in the vicinity of FTLs is not seen in many of the NFT-like intracellular tau deposits in CA1. Both MAP2 loss and increased NFT formation is potentiated in the vicinity of A beta-positive SPs.**

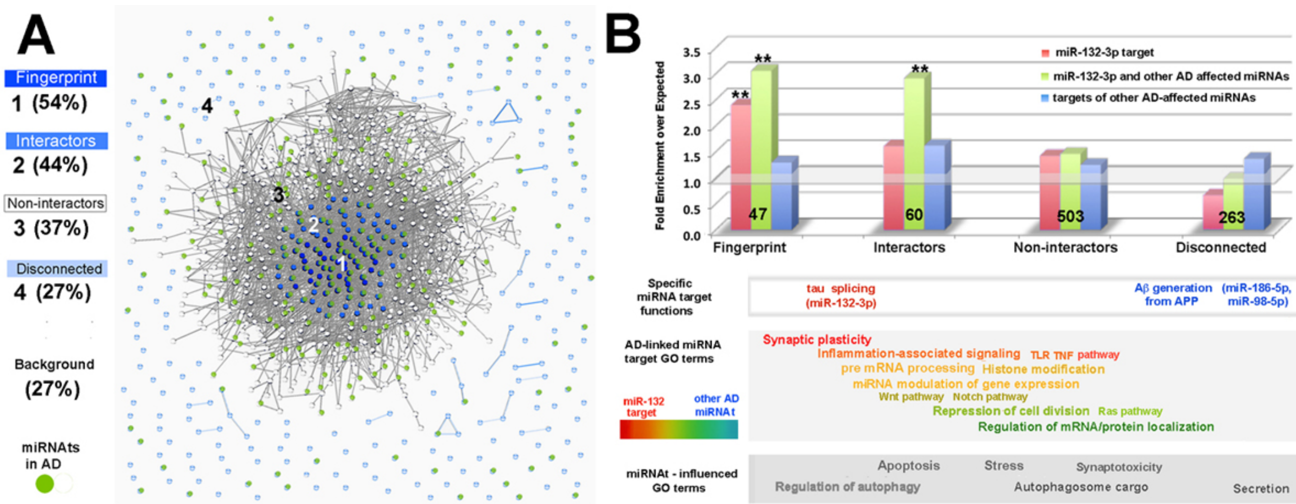

Figure 8: Targets of miR-132-3p and other AD-associated miRNAs play central functional roles in the multi-patient AD Stage 4 CSF EMV proteome. The 876 member multi-patient EMV 30-200 proteome from Stage 4 AD cases was subdivided into 4 classes based on functional interactions (String: coexpression, experiment, colocalization, datamining, moderate (0.4) stringency). These were: the 47 member "fingerprint" set (1), an additional 63 functional interactors identified in 3 iterative searches (2), the remaining 503 members with intergroup functional interactions but not with fingerprint proteins (3) and the remaining 264 members that were not functionally connected with the others (4). **Panel A** shows the percentage of each subgroup that were identified as moderate or higher stringency targets (10+ cites – TargetScan) of miRNAs (miRNAts) identified as being downregulated in AD (Prasad et. al. 2017 – icons shown in green). An additional group of miRNAts identified as being significantly upregulated (de-repressed) in miR-132 3p knockout tg mice relative to congenic controls (Hansen et. al. 2016) were also included in this analysis. We found that approximately 35% of the Stage 4 EMV CSF proteome were targets of 1 or more of these AD-modulated miRNAs and that functionally interacting, Aβ/tau-associated proteome members (Sets 1-2) are significantly enriched in miRNAts of AD-sensitive mi-RNAs relative to other functionally connected members (Set 3 - p ~ 0.01, Fisher's Exact Test). Each of Sets 1, 2 and 3 were also significantly enriched in AD-associated miRNAts relative to background (both $p < 0.0001$, chi square test). By contrast, non-interacting members of the proteome (Set 4) were not enriched relative to background (27% expected) and were significantly depleted in AD-modulated miRNAts relative to Set 3 ($p < 0.001$). **Panel B**: Comparison of miR132-3p targets with those of other AD modulated miRNAs in the Stage 4 EMV 30-200 proteome show selective enrichment of miR-132-3p targets relative to others, especially among miRNAts common to both sets (top). **Center, top:** In a separate analysis, targets of miR-98-5p and 186-5p, the disruption of which results in increased Aβ generation in AD (Hebert et. al. 2013, Kim et. al. 2015) in the BCSF4 proteome were found to yield a pattern that was virtually identical to that of the other (non miR-132-3p) AD-affected miRNA targets (15-5p, 512-3p, 29-3p, 212-5p, 219-5p). GO term analysis showed selective enrichment of miR-132-3p targets with CNS functions known to be affected in AD, including miR-186-5p and miR-98-5p targets. **Bottom, light background:** GO functions that were particularly enriched in AD-affected miRNAts are shown in bright color (high saturation, light background), with specific enrichment in miR-132 targets shown in red, non-miR-132 targets in blue and targets enriched in both (common) as yellows and greens. Overall, we found that miR-132-3p targets in the BCSF4 EMV 30-200 proteome were particularly linked to AD-disrupted functions (synaptic plasticity, inflammation) identified in other studies (Gupta et. al. 2015, Milan 2017). **Bottom dark background:** Functions that were enriched in both miRNAts and non-miRNAt Stage 4 EMV 30-200 proteome members (miRNA-influenced GO terms – shown low saturation). These functions as a consequence of upstream Aβ/tau-associated and/or miRNAt mediated dysfunction that diverted these proteins to CSF EMVs.

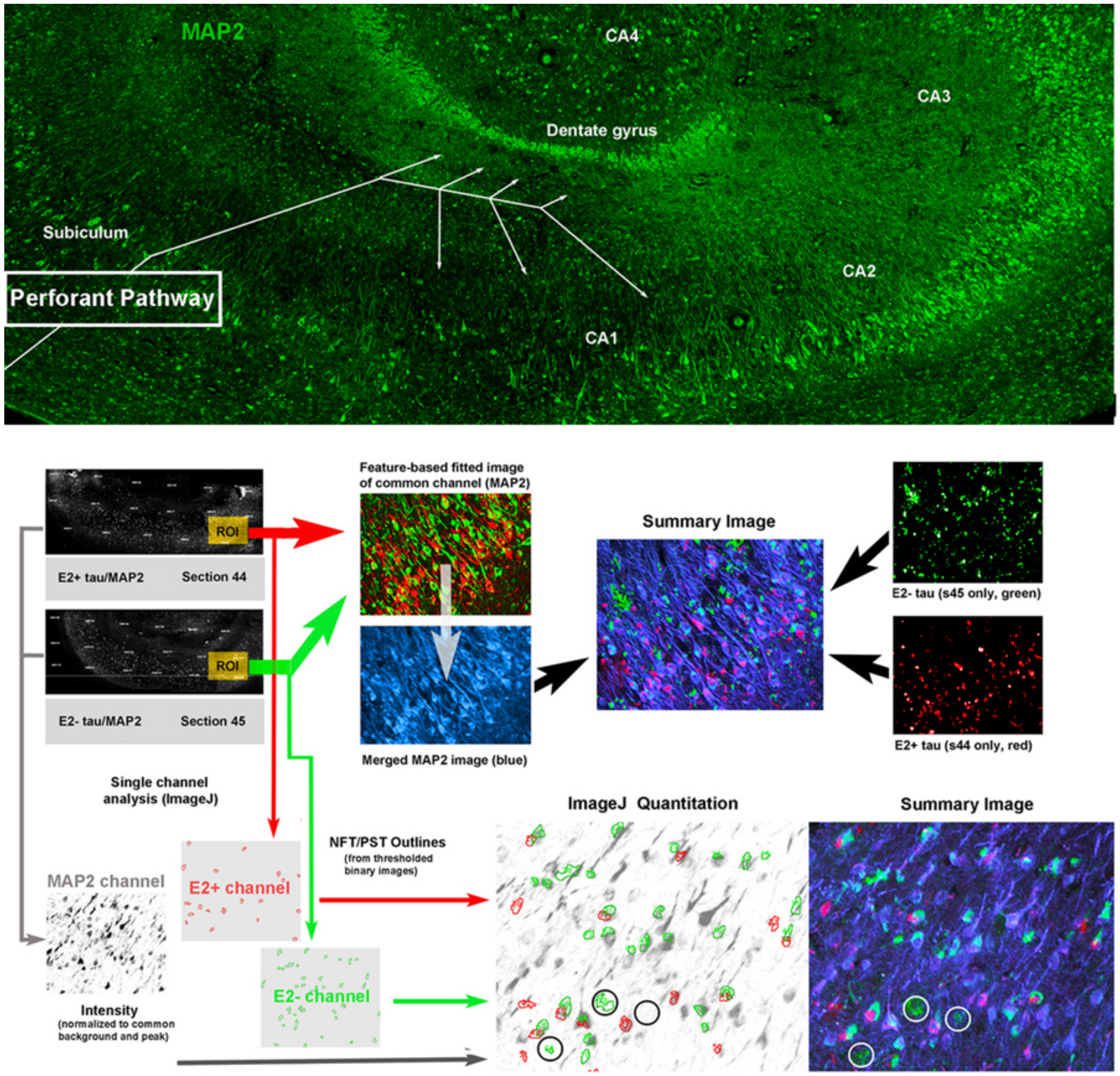

Figure 9 **Photomontaging and quantitative characterization of neurofibrillary (NFT) and diffuse postsynaptic (PST) tau lesion immunolabel in AD and CTE hippocampus** **Top:** A photomontage of a MAP2 immunolabeled hippocampal section from a Stage 5 AD case illustrates the regions of interest (ROIs) covered in this report. We focused on 2 major synaptic targets of the perforant pathway (white arrows) that show preferential neurodegeneration during the course of AD. These are the molecular layer of the dentate gyrus and the apical dendrites of pyramidal neurons in CA1 and the neighboring subiculum. Note that there has already been severe loss of MAP2 label in these areas in this patient. Other architecturally similar areas (CA2-3) that are relatively spared in AD (e.g. CA2-3) served as internal controls. **Bottom:** Photomantages of through the hippocamal region of 2 early AD (Braak stages 2-3) and 2 established AD cases were prepared as shown above to permit of the distribution, frequency of occurrence and MAP2 colocalization of NFTs and PST lesions. This approach is particularly useful for quantitative comparison of incompatable immunolalels (e.g. 9A1 and DC39) on adjacent sections that share common cellular elements that can be fitted together to generate a merged image when immunolabelled for a common cellular marker (MAP2). The generation of a summary image showing both E2- and E2+ immunolabel and their relationships with MAP2 label (top) and distribution and colocalization analysis of single channels (bottom) for a particular region of interest (ROI) from one of the Braak 5 cases is shown. Maps of E2- and E2+ lesion profiles from thresholded (binary) single channel images that were normalized to common background and peak intensity levels (using the "Levels" function in Photoshop) were then produced using the ImageJ "Analyze Particles" pulldown function. For colocalization analysis, E2- and E2+ immunolabel with MAP2, lesion profile maps were combined with normalized intensity based images of the combined MAP2 channel (gray), and the MAP2 intensities colocalizing with each lesion determined (ImageJ Analyze Particles).

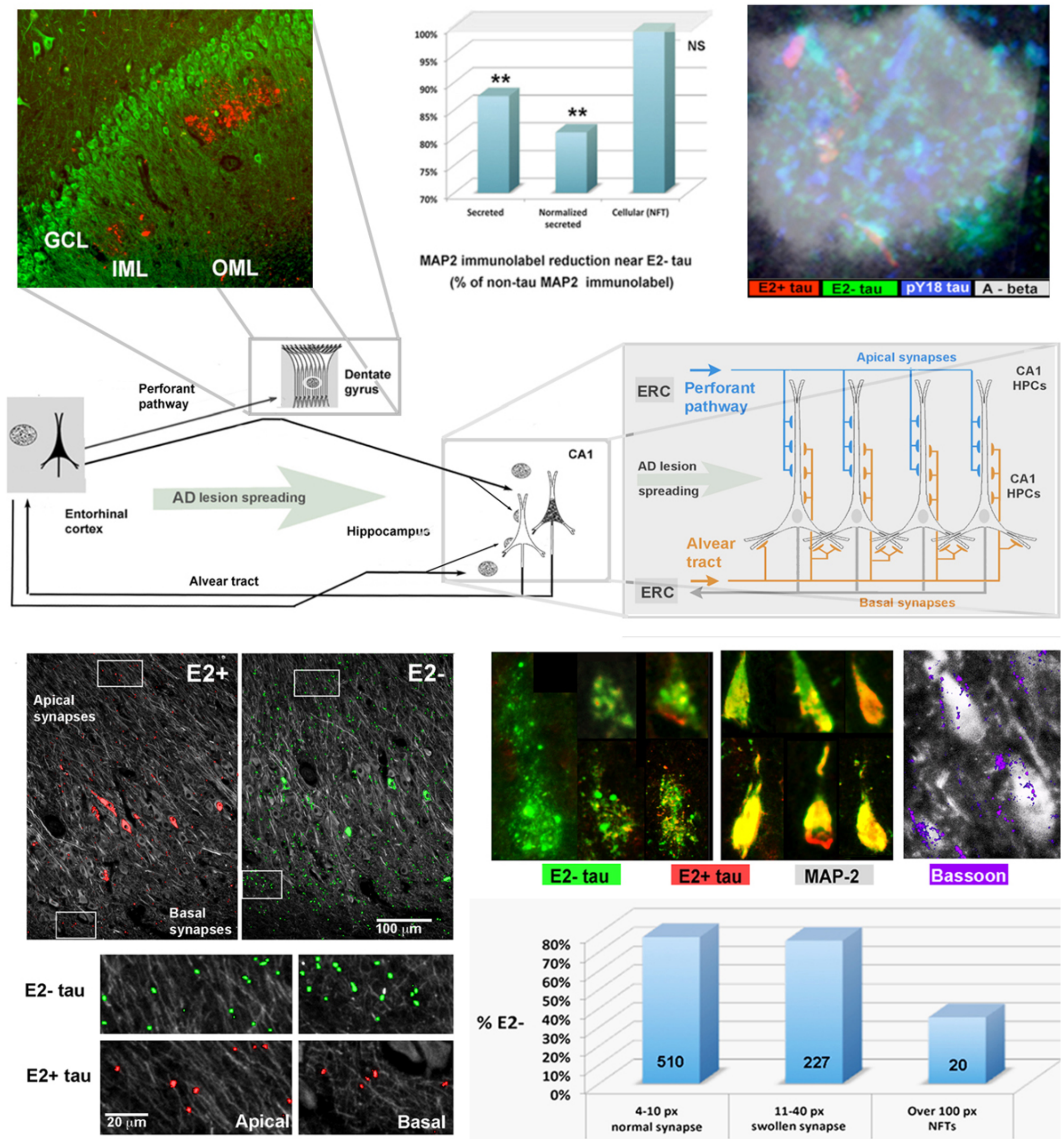

Figure 10 Schematic of perforant pathway projections from the entorhinal cortex (EC) to the dentate gyrus (DG), CA1 and subiculum of the hippocampus (HC) is shown (center), with images summarizing key features of E2- specific neurofibrillary lesion development in the dentate gyrus (top) and pyramidal cells of CA1 (bottom). Additional features of E2- specific features are shown in Figure 11. Well established features of PP circuitry include direct unidirectional connectivity between the EC and along which neurofibrillary lesion spread occurs in AD. EC connectivity to the HC via the PP projection to the molecular layer of the DG and apical dendrites of CA1 pyramidal neurons is exclusively afferent. The DG granule cell dendrites have no other direct link to the EC, whereas CA1 is also connected via pyramidal neuron efferents and ERC afferents via the alveus. The almost total absence of NFT-like tau deposits in DG granule cells suggests that FTLs in the dentate molecular layers are purely due to anterograde tau transport and secretion from axons and axon terminals originating in the EC, whereas CA1 tau lesions include NFTs and may be the result of both afferent and efferent connectivity. **Top panels:** Interstitial tau deposits in the dendritic fields of dentate granule cells in AD hippocampus are composed predominantly of E2- isoforms and appear to be toxic to local dendrites, since “holes” in MAP2 immunolabel in the GC dendrites E2- tau-positive FTLs (left).This was quantitated using ImageJ to compare immunolabel density (center) **Top Right:** Composite image derived from adjacent sections through an SP in the dentate molecular layer, showing co-extensivity of Abeta (white overlay) and E2- (green) but not E2+ immunolabel. SP-associated E2- tau lesions are accompanied by the phosphorylation of an N terminal tyrosine of tau (pY18 – blue). **Bottom Left:** Tau lesion spreading into the hippocampus proper (CA1) appears in the apical and basal dendritic fields of hippocampal pyramidal cells (HPCs) from PP and alvear tract axons, respectively This is associated with presynaptic terminal (PST) swelling of (primarily) E2- tau immunopositive PSTs (see graph at right) **Bottom Right:** CA1 HPCs contain what appear to be presynaptically derived intracellular accumulations of primarily E2- tau (D, left) as well as incipient classic NFTs (right). mAbs against the PST marker protein Bassoon and NFT phosphotau (AT-180) were used to verify PSTs and pre-NFTs in the Braak stage 2-3 AD cases shown here.

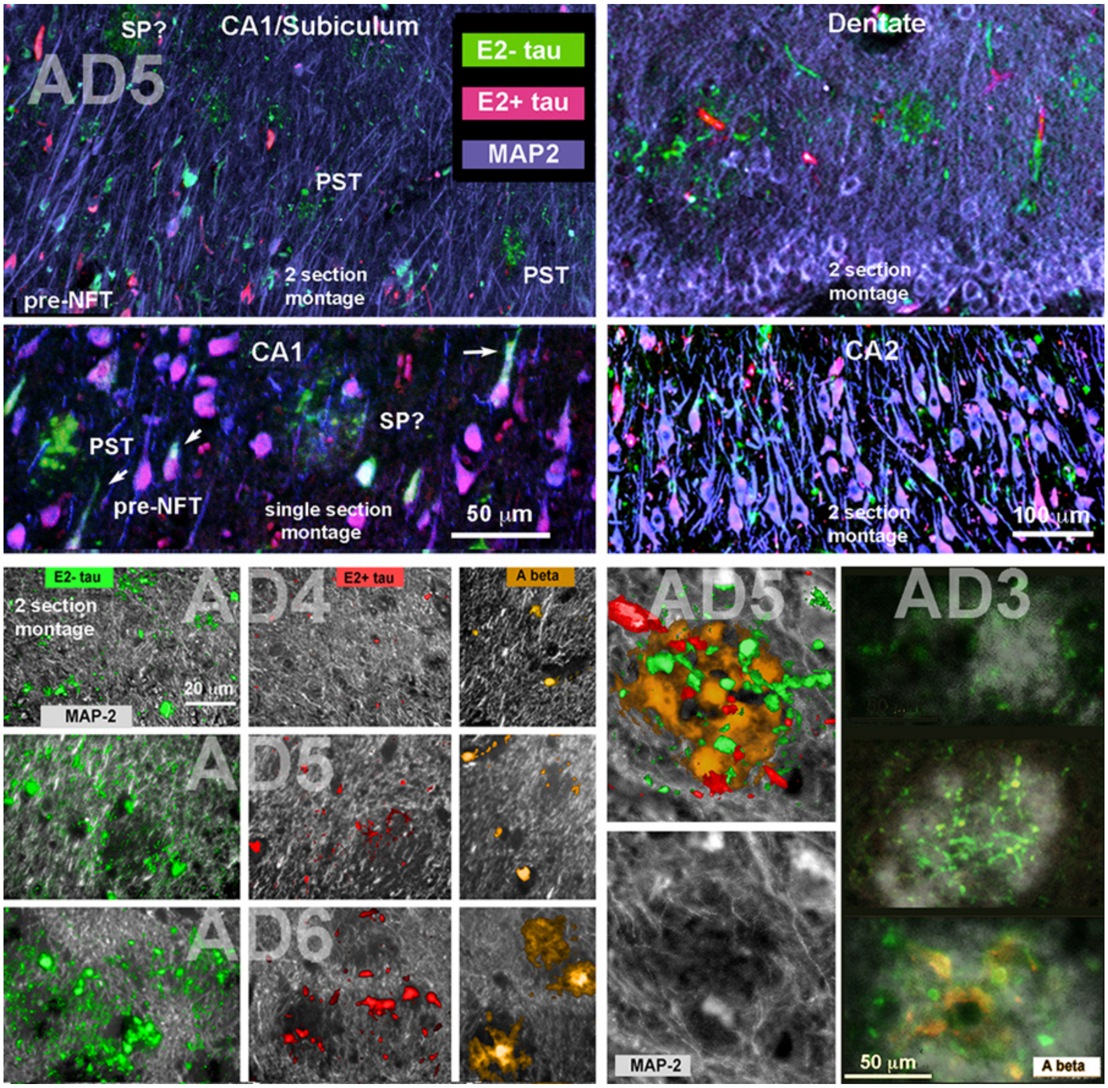

Figure 11 **A comparison of E2- and E2+ tau immunolabeling of hippocampal NFTs and "flocculent" tau lesions (FTLs) in AD Top panels:** Images are taken from adjacent section photomontages described in Figure 9 (top images, bottom right image). We also show an image from a more recent single section photomontage (bottom left). The CA2 panel is shown as an internal control, since it is typically spared significant neurodegeneration in early and moderate AD. FTLs in apical dendritic fields of CA1/subicullar pyramidal neurons can be SP-associated or SP-independent. This is not directly shown here (no channel was used for A beta immunolabeling) but is likely true of the larger FTLs that are similar in size to SPs (SP?) – also see Figure 13 for additional examples. These "plaque-like" FTLs closely resemble the FTLs described in the DG (Figure 10, top), and may (or may not) be associated with A beta positive SPs; others appear to represent swollen PP presynaptic terminals and are described more completely in Figure 10. The latter are typically SP-independent and appear to arise from presynaptic terminals impinging on somatodendritic pyramidal neuron profiles (right), and were E2- tau (green) and 9G3+ (PY-18) tau immunopositive (red). While both SP and non SP-associated FTLs are associated with PP presynaptic terminals, it is not yet clear to what degree their pathogenesis is related to each other and/or that of NFTs. **Bottom Left:** E2- tau dominant "flocculent" tau lesions (FTLs) develop in in the molecular layer of the dentate gyrus over the course of AD. This occurs in the absence of NFT development in granule cells and before the development of Abeta positive senile plaque-like lesions. We correlated the distribution of E2-, E2+ and A beta deposits with the progressive loss of immunolabel from foci within dendritic fields of granule cell neurons over the course of lesion development in AD. The MAP2 depleted halo in the granule cell dendritic field associated with FTL development correlates positively with Braak stage. **Bottom Right- left images:** More mature SPs tend to be associated with both FTL E2- positive and E2+ tau deposits (seen here as yellow - top) and are associated with localized MAP2 loss (bottom) especially in late stages (Braak stages 5-6). Higher Abeta immunolabel densities were associated with larger neuritic swellings, which were both E2- and E2+ tau immunopositive. **Right images:** In the CA1, SP development from small diffuse structures to large, neuritically invested ones is correlated with an early association with extracellular "flocculent" tau that is typically E2- positive. "Diffuse" SPs associated with predominantly E2- tau (top), and diffuse Abeta deposits (white overlay).

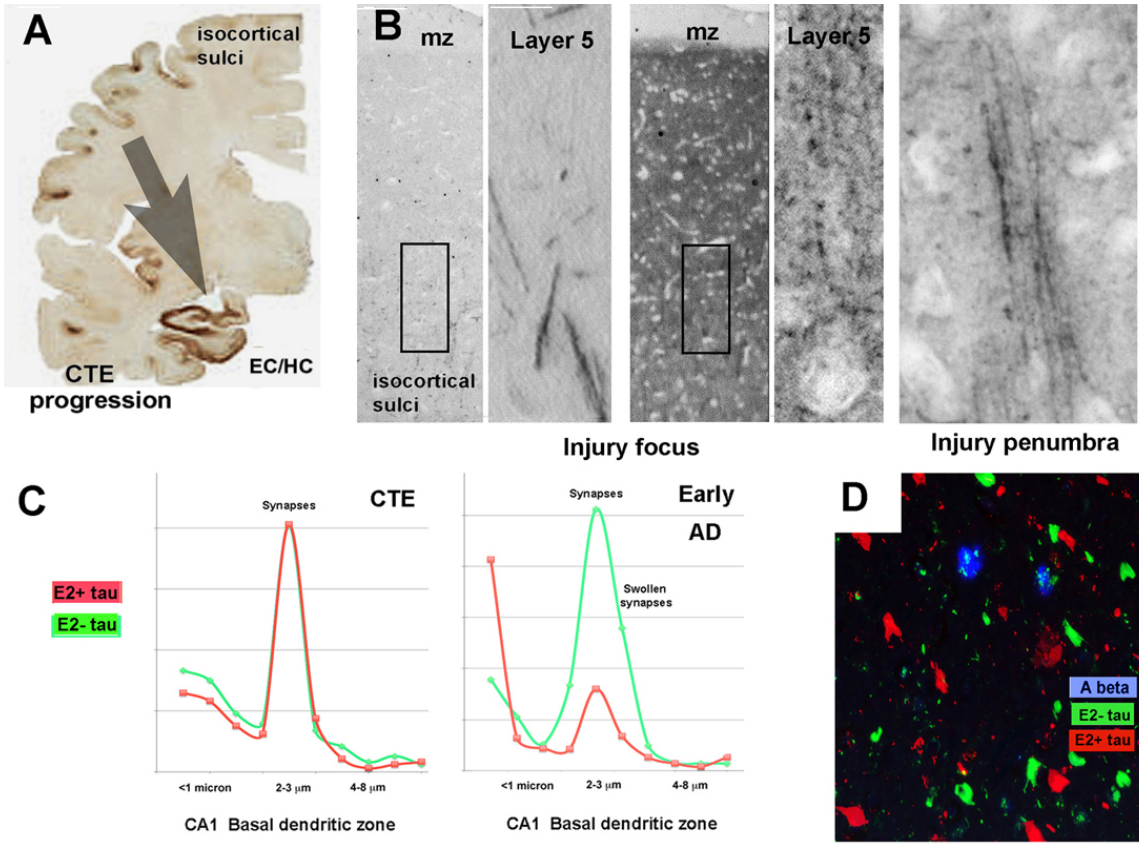

Figure 12 Tau lesions at primary (sulcal) and secondary (CA1 hippocampal) sites in CTE. Panel A: Lesion progression from primary lesion foci in isocortical sulci (Stages 1-2) to the ERC and hippocampus (Stage 3) in CTE. **Panel B:** In all of the diffuse isocortical sulcal tau lesion foci we have examined so far, E2- tau has been the dominant tau species; the presence of axonal and presynaptic terminal localized E2- label in penumbral isocortical lesions (B, right) suggest that the interstitial tau label is axonally derived. NFTs in both isocortical sulcal foci and in the CA1 were immunopositive for both E2- and E2+ isoforms resembled those seen in AD CA1, subiculum and in isocortex (not shown). **Panel C**: Inputs to the basal dendrites of CA1 HPCs do not show the E2-correlated changes in size and immunopositivity in Stage 3 CTE that we found in AD. **Panel D:** Some A beta positive plaques at both the primary sulcal injury sites (not shown) and in the CA1 (a secondary propagation site) showed the same E2- dominated neuritic halo as in AD, others did not. Despite the E2- specific association shown in D, it remains unclear whether there is any significant association of E2- tau deposits with PST swelling or cytotoxicity in CA1 owing to the small number of CA1 Abeta deposits so far in CTE cases.

(Summary of reported results, continued) These results are consistent with the results of Aim 1A, which indicate enrichment of upregulated genes associated with inflammation/immune activation and with current literature suggesting a role for presynaptic tau in early AD pathogenesis in association with Abeta. They are remarkable in 1) their clear identification of E2-, fyn-phosphorylated (i.e. 9G3 positive) tau species as the earliest form of tau deposited, 2) the strong correlation with localized neurotoxicity (MAP2 loss) and 3) the frequent appearance of E2- interstitial tau in plaque-shaped deposits in advance of any identifiable A beta immunolabel, especially in early stage cases (AD 2/3). This last point is highlighted by the frequent observation of swollen PSTs containing predominantly E2- tau surrounding HPC somata in CA1/subiculum in all stages of AD. Such lesions are apparently toxic, since they are surrounded by low MAP2 immunolabel, but are not plaque-shaped and do not co-clocalize with A beta. Collectively, these findings indicate that E2- tau species may have a specific and different interaction with A beta, and that this difference is important to A beta toxicity in AD. This is a major reason for our concentration on the tau-A beta link in subsequent studies as described below.

1B Summary of new data obtained and analyses performed during the NCE We have now completed the comparative characterization of FTLs in the DG molecular layers and CA1 pyramidal cell dendritic fields reported previously, and have confirmed initial qualitative observations with some quantitative work, examples of which are described below. The replacement of DC39 with 4G11, a more sensitive mAb with equal specificity for E2/3+ tau isoforms, was accomplished during the NCE and required us to validate/correlate earlier DC39-based results with current 4G11-immunolabeled material (not shown). 4G11 immunolabel recapitulated earlier DC39-based results but in addition revealed the presence of diffuse somatodendritic E2+ specific tau in both dentate molecular layer and CA1 pyramidal neurons. This is consistent with earlier literature on isoform-specific tau distribution in the CNS (Li et. al 2016) and led to additional characterization of E2/3 modulated distribution changes of tau in AD, which we have correlated with similar changes obserbed in propagated tau lesions in the dentate in CTE (Figure 13). An additional benefit of changing to 4G11 is that it is compatible with our E2- mAb (9A1) making it possible to double-stain single sections with E2- (9A1) and E2+ (4G11). The reason for the ability of 4G11 to bind to nuclear tau species much more strongly than DC39 might be due to its preferential labeling of 1N tau isoforms, which localize strongly to the nucleus. We have not as yet established this, but expect to do so in future biochemical studies.

Confirmation of earlier results obtained on adjacent sections We confirm most of the key results reported earlier that were obtained on adjacent sections, especially the characteristics of FTLs. These were: a) FTL association with swollen presynaptic terminals (PSTs) in both the dentate and in CA1, b) their E2- tau specificity in early stages, which evolved toward E2-/E2+ tau parity in more mature lesions, c) the absence of A beta deposits prior to the onset of FTL formation, especially in the dentate IML/OML and d) the selective correlation of local toxicity (MAP2 loss) with FTLs in both the dentate and in CA1. Lesion maturity was defined by the presence of diffuse vs neuritic A beta positive plaques. One finding reported earlier (the greater distality of cytoplasmic E2- tau in pyramidal cell somata in CA1/subiculum) appears somewhat less clear with 4G11, since the nuclear label.

Tissue samples and immunolabeling in the comparative CTE/AD study Most of the previously unreported work toward this Aim (i.e. during and since the beginning of the NCE) has involved the acquisition, immunolabeling, montaging and analysis of CTE (stages 3-4) and AD (stages 2-6) hippocampal tissue samples and the photomontaging of multiply immunolabeled sections on a HC-wide basis. We used an additional 8 samples from CTE1 cases (where tau lesion propagation to the hippocampus had not occurred) as general controls We have optimized imaging and montaging using a Zeiss AiryScan confocal microscope and a semiautomated montaging program (Zen Blue) at the Jamaica Plain MA VA Hospital confocal facility (in collaboration with Dr. Russ Huber), which we used to generate the material used in the AD-CTE comparison described below. Samples were usually triple immunolabeled using mAbs 4G11 (E2+ tau) and 9A1 (E2- tau) on all 204 sections processed (76 CTE3/4 and 128 AD 2-5), with the 3rd channel reserved for mAbs against 4 markers of interest i.e. 1) MAP2, 2) activated microglia (iba1), 3) beta amyloid, 4) all tau (H7) plus the nuclear marker DAPI. This resulted in 49 sections (16 CTE 3/4, 25 AD 2-5, 8 control) labeled for E2-, E2+ and each of the 5 markers listed above. In addition, we have recently tested a new E2- specific mAb (H36.H7) on 3 Stage 5 sections and found the staining pattern to be identical with that of 9A1.

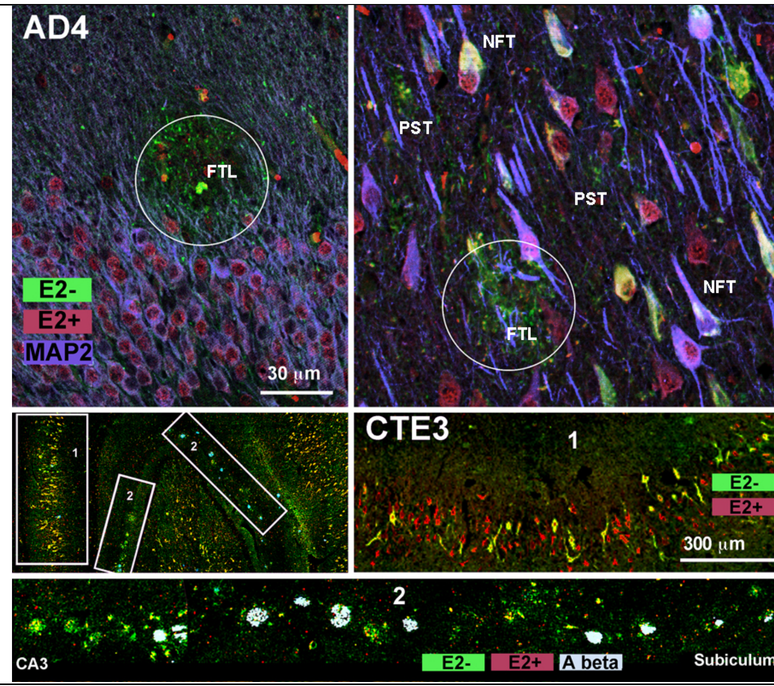

Figure 13 Findings resulting from 2 technical advances made during and since the NCE (9-30-2016 to date) Two technical changes a) use of 4G11 for E2+ tau instead of DC39 and b) semiautomated photomontaging have expanded and facilitated the comparative analysis of DG and CA1 lesions (top) and larger scale (HC wide) comparisons of both FTLs and NFTs (bottom). Top: What we have called FTLs in the DG closely resemble SP like lesions in CA1 in terms of E2- tau label, whether or not A beta immunolabel is present. Unlike the E2- lesions in the DG molecular layer, one can distinguish an additional smaller FTL-like lesion type made up of swollen PSTs in CA1 that is centered around the somata of individual pyramidal cells (PST). NFTs in CA1 largely resemble those in adjacent section images. Bottom: Comparisons of NFT distribution through the HC (1) and surveys of Abeta colocalization with FTLs throughout the dentate ML/GC stripe abutting HC regions extending from distal subiculum to CA3 (2) have been greatly facilitated by automated Zen Blue) photomontaging. Scale Bars are approximate.

Correlation of NFTs and FTL characteristics and development in AD and CTE Our approach to characterizing CTE lesions has been informed by the results reported for AD hippocampus. Since the spreading to the EC and HC in CTE superficially resembles that of AD (McKee et. al 2013), resulting in a “secondary” type lesion dependent on propagation rather than direct physical injury, we have focused on higher stage (III and IV) CTE HC samples for tau lesions that can be characterized in terms of the E2- and E2+ tau–specific features that we have identified in the parts of the HC that we focused on for characterizing the development of E2- tau lesions in AD.
Most of the analysis presented below therefore involves a comparison of the 2 tau lesions characterized earlier – i.e. the largely E2- dominant flocculent tau lesions (FTLs) and NFTs in 2 loci – i.e. the granule cell and outer/inner molecular layers of the dentate gyrus and the pyramidal cell layer of CA1 in disease stages where hippocampal changes are either incipient (CTE3, AD2/3) or established (CTE4, AD4/5). Because of the very low incidence of CA1 FTLs (both SP-like and PST-only cellular profiles), we have devoted most of our effort to comparing propagated tau lesions in AD and CTE to the dentate gyrus (DG) molecular layers, where plaquelike FTLs with and without localized A beta deposits occur in both AD and CTE. The results of all AD-CTE comparative analyses are summarized as bullet points below, followed by a more detailed account of the correlation analysis of dentate FTLs with localized A beta label in AD versus CTE.

- **Nuclear E2+ tau** There is a progressive change in the distribution of E2+ (4G11+ tau) is the somata of GCs during the course of both AD and CTE, with progressive displacement of nuclear E2+ tau label that is prominent in incipient AD (Stages 2-3) to the perinuclear cytoplasm by Stage 5 (Figure 14). However, we have not yet observed the transient increase in E2+ tau nuclear label seen in Stage 2 AD in any CTE cases, suggesting that this feature may be AD-specific. E2+ tau nuclear label is also prominent in Stage 4 CA1 pyramidal neurons, but it is unclear whether it is cleared progressively with increasing stage as it is in the dentate in either AD or CTE (Figures 11, 13)

- **FTLs in the DG are more colocalized with activated MGs in CTE than AD** FTL-like E2- tau lesions form in the dentate molecular layer in both AD and CTE. These appear to be identical in

E2- specificity and size, both with respect to the diffuse tau fields and the size profile of swollen terminals. Both are accompanied by significant local MAP2 loss and both appear to serve as foci for microglial localization and activation, although this appears to be more prominent in CTE (Figure 15). CT3/4 samples exhibited significantly more specific E2- containing nucleated (DAPI positive) glial-like profiles in the vicinity of FTLs than elsewhere in DG molecular layers, which were dominated by E2+ positive nucleated profiles, a result not seen in AD cases (Figure 16). We interpret this as evidence that inflammatory changes in CTE may be distinct in nature from those accompanying AD.

- **A beta positive senile plaques in CTE and AD** We have identified numerous plaque-like Abeta deposits in the vicinity of FTLs in the dentate molecular layer in CTE3/4 samples. As with AD, we found E2- FTLs occurring in the absence of localized Abeta immunopositivity, but not the reverse, a result that emphasizes the importance of E2- tau species in the early pathogenesis of both AD and CT in the hippocampus. By contrast, we have not yet identified any definable differences in senile plaque-associated lesion development or toxicity in CA1 between AD and CTE (not shown). This is likely due to intersubject variability and relative paucity of SP-like lesions in CA1 in CTE 3/4.

- **Other CTE/AD comparisons** We have observed greatly increased E2- positivity in small neuron-like cells near the hippocampal fissure in a significant majority of CTE3/4 cases (10 of 14) relative to equivalent stage AD (3 of 12).

The occurrence and significance of A beta-containing SP-like lesions in CTE pathogenesis is far more controversial than it is in AD, where A beta production is generally accepted to play a central role (McKee et. al. 2013, Rapoport et. al. 2002, Ittner et. al. 2010). Somewhat surprisingly, we found significant SP lesion loads in most of our CTE3/4 samples. More of the CTE3/4 A beta-containing SP-like deposits were localized to the dentate than to CA1 (an example is shown in inset 1, bottom of Figure 13). This pattern was unlike our AD cases, where most SPs were localized to the HC "proper" (i.e. CA1-4) and adjacent subiculum, with only a minority in the DG. When present, SPs in the DG molecular layers colocalized with some, but not all molecular layer FTLs in both CTE3/4 and AD samples. Since perisynaptic A beta plays an established role in localized tau misprocessing that is mediated by the tau N terminal domain in AD, but not CTE, this presented us with a major opportunity for a fruitful comparative analysis of tau propagation mechanisms to the DG in CTE vs AD.

We found proportionally more large, irregular cell-like profiles in CTE 3/4 cases than in equivalent AD stages (4/5), with significantly more nucleus (DAPI) positive profiles present in CTE molecular layers (as a proportion of total field area) than in AD, apparently due to activated microglial (AMG) recruitment (Figures 15-16). This suggests that FTL formation with the onset of tau lesion propagation to the dentate in CTE has a stronger contribution of inflammation-related mechanisms than is true of the equivalent stage in AD, causing disproportionate AMG ingestion of E2- tau near FTLs (Figures 15-16). However, in CTE it is unclear if this is caused by the presence of A beta deposits (as is commonly assumed to be the case in AD), or if A beta deposition and E2- tau deposits are themselves a consequence of axonal disruption, possibly directly involving the PP itself. In the latter case, selective AMG recruitment to FTLs might simply be a consequence of Wallerian degeneration of injured PP axons. We have found that primary CTE sulcal isocortical tau interstitial deposits consist primarily of E2- tau that has (apparently) been released by injured axons of passage (Figure 12B), and both tau and A beta accumulation in axonal profiles is an established response to axonal injury in acute TBI (Uryu et. al. 2007). Since HC involvement is usually absent in early/mild stages (1 and 2) of CTE, we have assumed that Wallerian degeneration in the PP is not

a factor in moleculat layer FTL formation in CTE 3/4, but this possibility has not yet been explicitly excluded, and remains a future direction of research. We chose instead to comparatively assess the relative predominance of E2- vs E2+ tau immunolabel ratio in terms of the intensity of co-localized A beta immunolabel in DG molecular layer FTLs in CTE3/4 and AD 4/5 cases. This was done quantitatively on A beta labeled sections using ImageJ-based size analysis of thresholded PST profiles using the "analyze particles" pulldown on PSTs within each FTL, comparing A beta associated with non-A beta associated FTL profiles (Figure 17). Correlation of immunolabel density was performed on non-thresholded, single section montage images of 4G11 and 9A1 immunolabeled FTLs under a thresholded mask made from the third channel A beta immunolabel.

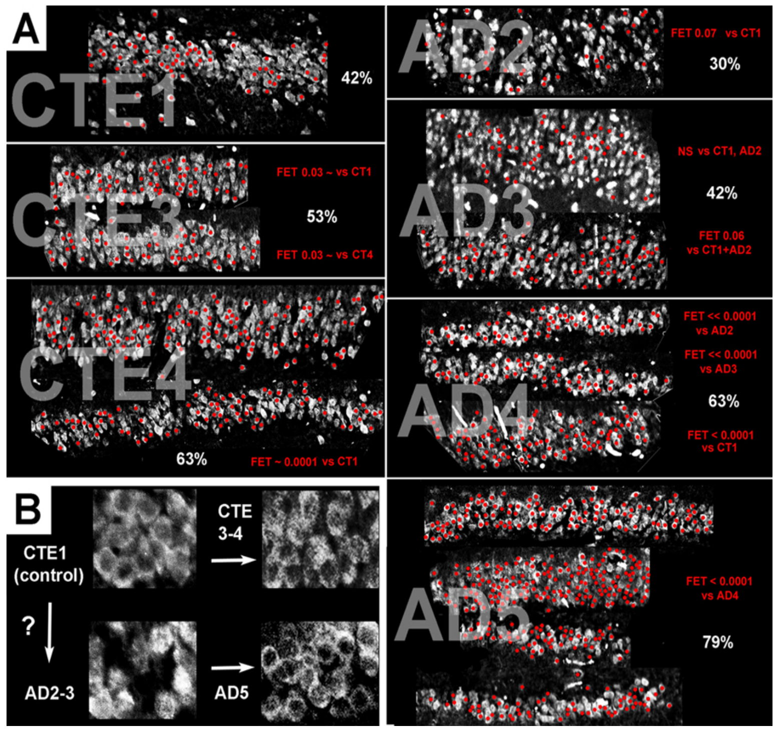

Figure 14 Significant changes in E2+ cellular staining patterns in DG granule cells occur with CTE and AD pathogenesis Panel A: Quantitative densitometric comparisons between 4G11 immunolabel in nuclear profiles vs surrounding cytoplasm were performed using ImageJ, with all nuclei having less than 50% as much 4G11 label as the surrounding cytoplasm marked (integrated density of area under DAPI positive or MAP2 negative mask – red circles). The significance of differences between marked and unmarked GCs in sets of GC layers and CTE1 (used here as a control) was calculated using Fisher's Exact Test (Vassarstats – 2x2 array). In both CTE and AD, there was a significant clearing of E2+ tau immunolabel from nuclear profiles with disease progression, suggesting that displacement of E2+ tau isoforms from the nucleus is a common feature. Very early stages of AD show a marginal increase over control(p~ 0.07, FET). **Panel B:** High resolution comparison of the progressive nuclear clearing of 4G11 immunolabel in GC nuclei from AD vs CTE suggests that increased nuclear E2+ tau occurs in very early stages of AD. E2+ nuclear label is punctate, except in those AD2 cases where nuclear label is increased relative to controls and later stages.

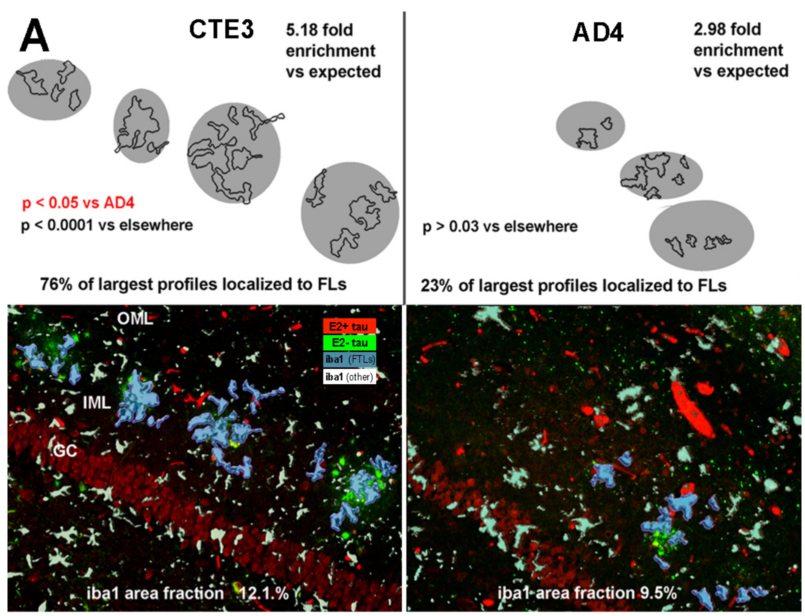

Figure 15 CTE and AD give rise to distinctive microglial activation patterns in the dentate gyrus The similarity of E2- dominant flocculent tau lesions (FTLs) propagated to the hippocampus in CTE and AD can best be seen in the dentate gyrus, where FTLs (consisting of diffuse extracellular E2- tau deposits) form in the outer and inner molecular layers (OML/IML) near swollen perforant pathway presynaptic termini. In both CTE and AD, these are associated with localized cytotoxicity (MAP2 loss) in granule cell (GC) dendritic fields. ImageJ comparative analysis of iba1 profile number, size and circularity shows a greater localization of large, low circularity profiles near FTLs (top, shaded outlines) in CTE vs AD, but also significant localization vs expected in AD. Calculations are for the sections shown(bottom), but similar results were found in other iba1 labeled sections, some of which (i.e. for AD) have been reported previously. OML = outer molecular layer, IML = inner molecular layer, GC = granule cell.

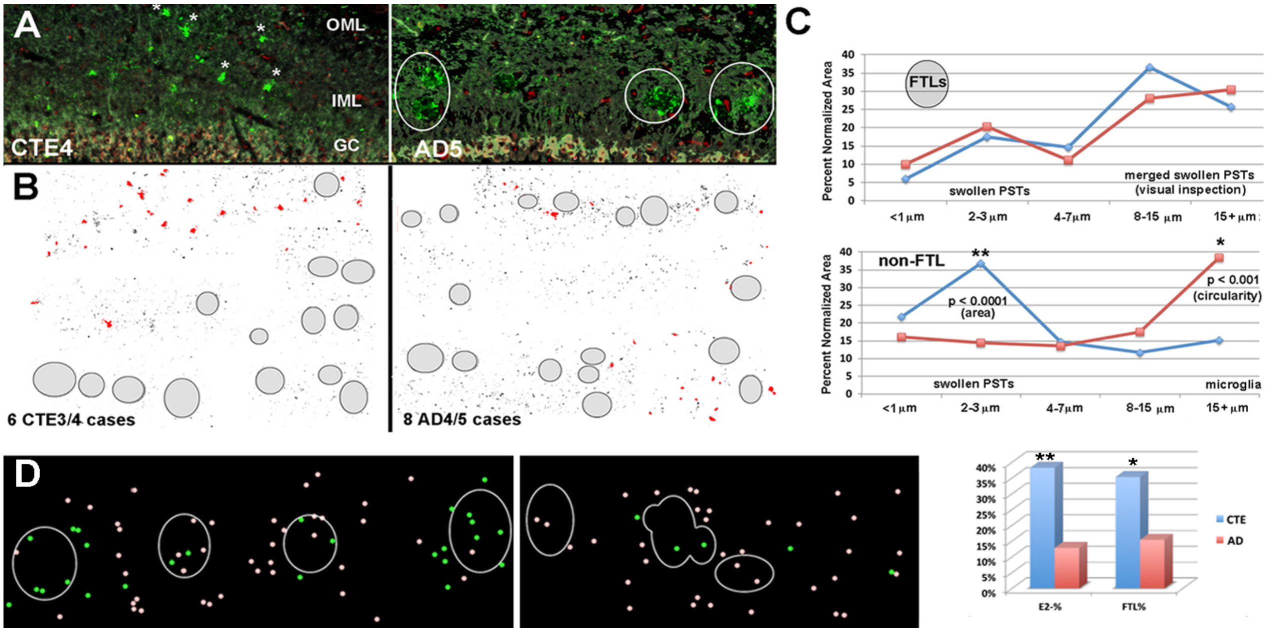

Figure 16 CTE and AD E2- tau profiles in the dentate molecular layers are similar within FTLs, but differ significantly elsewhere. **Panel A:** Sections from established CTE (left) and AD (right) stages show distinctive E2- tau lesions that resemble activated microglia (AMGs) that have expressed or endocytosed tau (asterisks) as well as extracellular accumulations of E2- tau in the vicinity of swollen PSTs (circles). **Panel B:** Composite images of thresholded E2- immunolabel in from dentate molecular layer fields of multiple CTE (left) and AD (right) cases, showing the size and shape range of E2- tau deposits observed in our study. Oval outlines show FTL-like lesions similar to those in Panel A. Shape characteristics of a subset of larger profiles (8 square microns in area or more) are shown in red. **Panel C:** Top: FTLs in CTE (red) and AD (blue) had similar PST-like profile sizes. Data were derived from ImageJ analysis of the composites shown in B, which yielded 284 and 475 profiles in CTE and AD, respectively. In FTLs, all profiles appeared to represent PSTs, with the larger ones representing multiple terminals which were merged in the thresholded image. By contrast, E2- profiles in OML/IML regions outside of FTL perimeters showed distinctive features, with a significantly higher number of PST-like profiles with high circularity in the AD cases. Non FTL regions in CTE samples showed a larger proportion of very large E2- profiles than AD samples that represent glial cells, mostly AMGs, which also showed significantly lower circularity values than PSTs. Significance tests were based on distributional differences in profile size category (area - Fisher's Exact Test, 2 tails), or Student's T test (ImageJ circularity). **Panel D:** FTLs in CTE3 patient molecular layers (left) exhibited more DAPI positive profiles (nuclei) of tau-positive phagocytic cells than equivalent AD (Stage 4) samples (center), and also have more E2- positive cellular profiles, both in the vicinity of FTLs and elsewhere in the molecular layer (right). OML = outer molecular layer, IML = inner molecular layer, GC = granule cell.

Figure 17 Size and nature of E2+ and E2- profiles in FTLs are differentially affected by local A beta deposits in CTE vs AD ImageJ particle analysis of the size distribution of E2- and E2+ tau isoforms within FTLs in the dentate shows distinctive disease and isoform-specific differences. The presence of local A beta correlates with a significant E2- specific increase in the size ($p \sim 0.01$, Student's T test) in the largest profile class in CTE (asterisk), but not AD, presumably due to AMG invasion of FTLs (see text). In AD, A beta is associated with increased E2- PST size (double asterisk), both by class distribution (FET: $p < 0.001$) and mean size (T test: $p < 0.0001$). A beta had no discernable association with E2+ profile sizes either in CTE or AD. However, E2+ profiles were significantly larger overall in AD than in CTE (triple asterisk, $p << 0.001$, Student's T test), mainly due to increases in the proportion of large profiles (FET $p < 0.0001$).

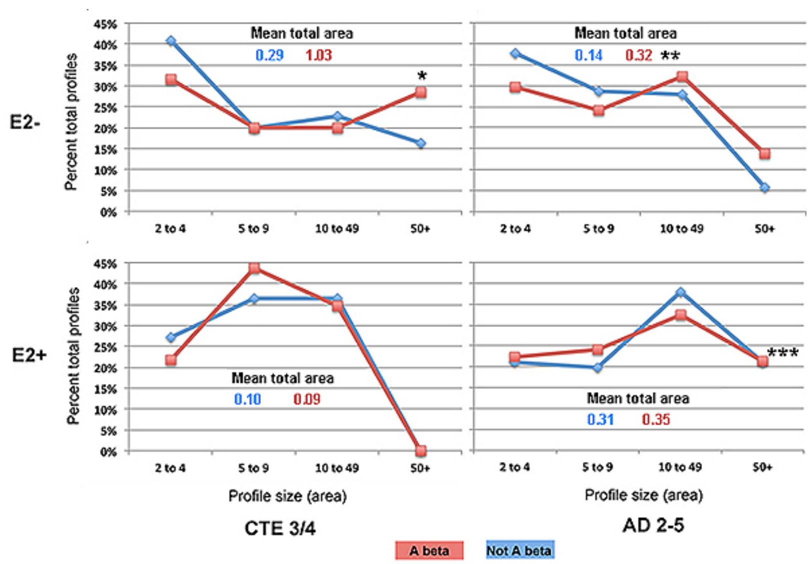

An unthresholded A beta image was then used to determine image density for A beta, which was then plotted against the ratio of E2-/E2+ immunolabel for each FTL (Figure 18). All density measurements were made using the ImageJ “measure” pulldown on images normalized to background.

We found that the size profiles of FTL-localized PSTs differed significantly between CTE and AD, with E2- profiles being larger than E2+ terminals in CTE, and the reverse being true in AD. both the mean total area and the largest size class being far larger/more prevalent in AD (Figure 17, triple asterisk). However, there was no discernable correlation with A beta label in PST terminal size, once the effect of DAPI-positive profiles (AMGs) was subtracted (*loc cit* single asterisk). In AD, we did find a clear positive correlation of A beta immunodensity with the presence of E2+ tau species in the FTLs as a whole (Figure 18, left graphs – shown as a negative slope correlation with E2-/E2+ ratio). This confirmed qualitative earlier reports in plaque-associated and plaque-like FTLs in CA1/subiculum (Figures 10 and 11), but was somewhat surprising in that increased E2+ signal was combined with a significant negative correlation of overall E2- immunolabel. This suggests an ongoing and relatively sensitive interaction between extracellular A-beta deposits and both the intracellular accumulation and secretion of N terminal-containing tau species, which is consistent with a key role for the tau projection domain in mediating A beta tau interactions in AD (King et. al. 2005, Ittner et. al. 2010). By contrast, we have not found significant correlations of N terminal isoform differences with A beta intensity in CTE cases. However, we have not yet analyzed as many CTE sample FTEs as we have for AD; this analysis is still ongoing.

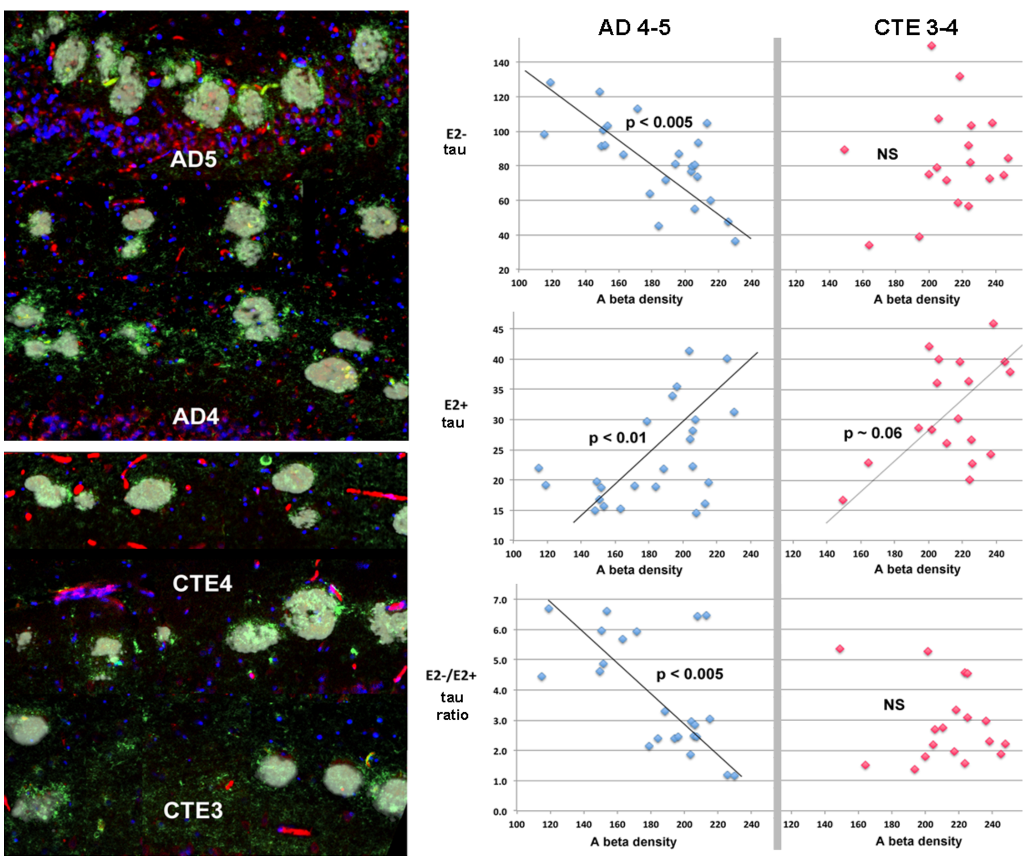

Figure 18 The amount of Abeta near FTLs in the DG is significantly correlated with the ratio of E2- to E2 interstitial tau at FTLs in AD than in CTE. Composite images (left) of A beta positive dentate gyrus FTLs in single section montages of AD (top) and CTE (bottom) samples labeled with 4G11 (E2+ specific (red) and 9A1 (E2-specific (green) and a mAb against A beta 1-42 (white overlay). DAPI label is shown in blue. The results of ImageJ density analysis for each channel on a per lesion basis (icons) is shown at right, with AD in blue (left) and CTE in pink (right). Note that significant correlations could only be identified in FTLs from AD cases.

Aim 2: 2A: Biochemical interactions between Tau & the exosomal proteome
2B: Cell culture and tissue based assays of isoform-specific tau internalization and cellular localization

2A/B Summary of previously reported results: In previous reports, we described an analysis of the effects of expression full length and N terminal half E2- and E2+ tau species in SH-SY5Y neuroblastoma cells on cell lysate exosome fraction proteomes obtained from by use of mass spectrometry to obtain high stringency thresholded datasets. A summary of E2- and E2+ specific exosomal proteomes with respect to tau, Abeta and TNF alpha (a key mediator of microglial-mediated inflammation) is shown in Figure 19. As mentioned in previous reports, we chose TNF alpha to facilitate comparisons with the parallel IHC studies using Iba1 reported above. We found that String 10.0 based interactomes for E2- specific exosomal proteomes linked tau, A beta and TNFa via multiple physical interactions involving mostly upregulated in AD proteins, many of which were identified in AD CSF exosomes. This was much less true of the E2+ specific SH SY5Y exosomal proteome (Figure 19).

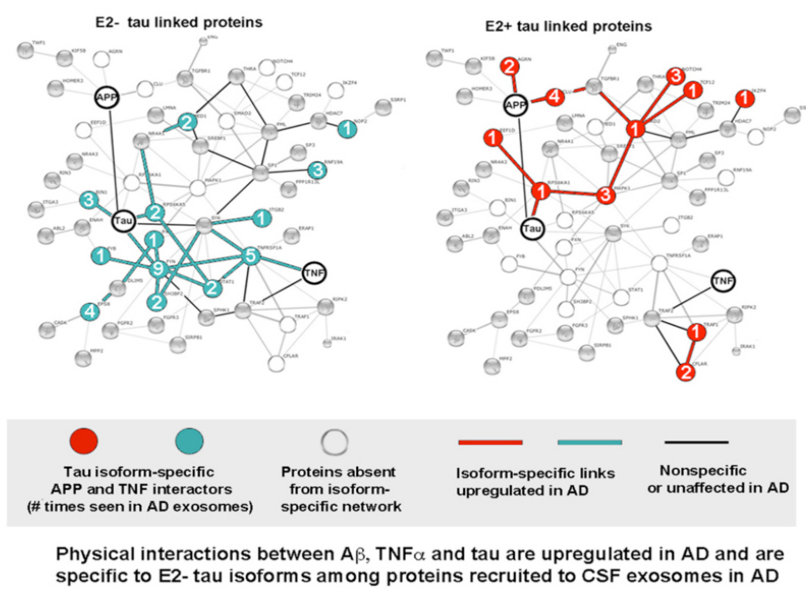

Figure 19 E2- tau isoform-specific interactions between tau and Ab via upregulated proteins with physical links to TNFa-associated inflammatory pathways. Proteins recruited to the exosomal fraction in SH-SY5Y cells interact with Ab-associated inflammation (TNF alpha) proteins in an E2-tau and AD specific pattern. Of the 1921 proteins identified by mass spec in SH SY5Y exosomal fractions with tau expression that were absent from the untransfected control proteome (1344 proteins), around 54% (1041) were unique to either E2- (530) or E2+ (511) tau isoform expression. Of these, 176 are upregulated in limbic lobe tissues during early AD (Antonell et. al. 2012, Blalock et. al. 2011, modified according to Talwar et. al. 2016), and of these, 131 have known physical interactions with one another and with tau, Abeta and TNFa. We used String 10.0 (Fransechini et. al. 2014) to generate a network diagram of the interactions between 69 "connected" proteins present in AD brain or CSF exosomes and found that the "E2- unique" proteins among them were significantly more connected to than did E2+ AD-affected proteins (blue vs red icons and links). This difference was specific to individual proteins (e.g. **TNFRSF1A, BIN1, FYN, RPS6KA5**) were present in our "fingerprint" (Figures 6-8).

We have also reported preliminary size profile data from tau uptake experiments (Figure 21B), which remain in progress. We had previously presented differential axonal and dendritic Tau and MAP2 localization and hoped to continue tau localization analyses using various neuroblastoma cell lines (P19, SH-SY5Ys, NB2As), but these have been frustrated by our inability to obtain cells that are sufficiently differentiated to localize distal dendritic and axonal components reliably and that can also be effectively transfected, and we have been forced to discontinue this work. We are not sure if the failure of differentiation was due to the toxicity brought by tau over-expression or due to the disruption of cell differentiation function brought by random tau sequence insertion to the genome. We did succeed in generating stably transfected cell lines (described below), which we have used in furtherance of other aspects of Aim 2B. Finally, we performed exploratory proteome

analyses of subcellular fractions of hippocampal homogenates of Stage 4 AD patients in an attempt to validate one of the underlying assumptions of this project – i.e. that upregulated proteins in early AD are localized to secretion pathways (endosomes, Golgi and endoplasmic reticulum) rather than to autophagosomes, which should contain downregulated proteins diverted to exosomes via exophagy (Abrahamsen & Stenmark, 2011). This idea was mostly validated and has been reported previously (Second Annual Report). It is not reproduced in this Final Report owing to space considerations and to the fact that its results (and our assumption) are now generally accepted by investigators in the field.

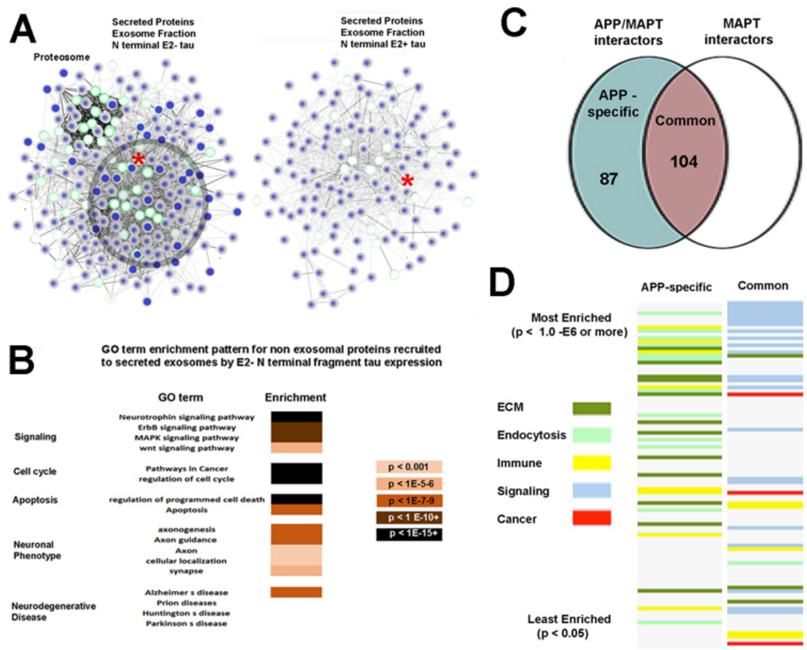

Figure 20 Analysis of secreted and modeled exosome fraction proteomes Panel A: Connectivity diagrams of known physical interactions (String 10.0) are shown for tau-interacting proteins (asterisk) identified in culture media exosome fractions. GO term (EE) members (green icons) and non EE proteins upregulated in AD with high connectivity (5+ links – blue icons) are indicated. The latter are found only in the secreted proteome from E2- tau expressing cultures; several were members of the "fingerprint" set identified in CSF analyses (Figure 7). Proteostasis-associated proteins (mostly EE members) are also selectively found in the E2- associated fraction. **Panel B:** GO term analysis of the E2- projection domain proteome reveals enrichment of many of the same functions identified as being AD-specific in multipatient CSF proteomes from early AD cases (Figures 2-4). Enrichment significances were taken as provided by String 10.0. **Panel C:** Venn diagram of our model of the effects of A beta on recruitment to exosomes by tau expression on secreted SH-SY5Y proteomes. This was modeled using String by determining the 104 intersecting (brown) and 87 non-tau interacting (blue) sets among all proteins known to interact with APP and/or tau (APP/MAPT) and of tau only (MAPT) directly at moderate strength or greater. **Panel D:** GO term enrichment profile of the comparison diagrammed in C. Note that expected APP-specific functions include extracellular matrix (ECM) interactions, endocytosis and immune-specific terms, but not signaling or cancer-specific terms.

2A Summary of new data obtained and analyses performed during the NCE We have repeated and expanded our earlier analysis of exosome fractions from cell lysates of tau-expressing SH-SY5Y cells to include secreted exosomes. This work (summarized in Figure 20) has yielded results that are broadly similar to our analyse of CSF exosome-containing fractions (EMV 30-200), but differ in some important details that are consistent with the model system being used. For instance, the large predominance of proteins whose expression is upregulated in AD was absent from both lysate and secreted exosomes. This is likely due to the absence of AD-associated changes in specific miRNA populations which may be required to "de-repress" AD-associated genes diverted to CSF exosome fractions. In addition, there was a moderate overrepresentation of cell cycle, cancer associated and apoptosis-related proteins relative to CSF, although all of these functions were enriched in AD CSF as well (see Figure 2). This is expected owing to the fact that the cells are themselves cancer cells (neuroblastoma-derived), and was reduced but not eliminated by subtracting all members of control (non tau expressing) proteomes from the analyses, possibly because these functions are common to both cancer and AD pathogenesis. However, the strong enrichment of specific tau-associated signaling pathways (MAPK, Wnt, NT and ErbB) was also noted in AD CSF, and there was even selective enrichment of the AD GO term relative to those of

other neurodegenerative diseases (Figure 20B). The most significant E2 isoform difference identified was obtained by expressing N terminal half constructs and was found in the secreted (i.e. culture media) exosome fraction among proteins that are not members of the "extracellular exosome" GO term – i.e among proteins recruited to exosomes. These proteins had far more comprehensive physical interactions with tau than did the proteins specific to the secreted proteome of E2+ projection domain expressing cultures (compare String diagrams in Figure 20A). This finding tends to confirm the major premise of this project – i.e. that the tau projection domain plays a critical role in AD- affected functions, especially in E2- tau isoforms. Finally, since we have found significant A beta associated differences in E2- and E2+ tau deposits in both AD and CTE (described in detail above and in Figures 11-12 and 17-18) we also performed a bioinformatic analysis directed at predicting expected A beta-specific features of GO term profiles using String 10.0 as described (Figure 20C and D). This was based on known protein-protein physical interactions between A beta (APP in String), tau (MAPT) and other proteins as curated from the literature and published databases. Completion of this work resulted in the awarding of 1 Masters of Science degree (Sarvani Manne) and forms a major portion of the thesis work of a current PhD student in my lab (Mohammed Aladwan).

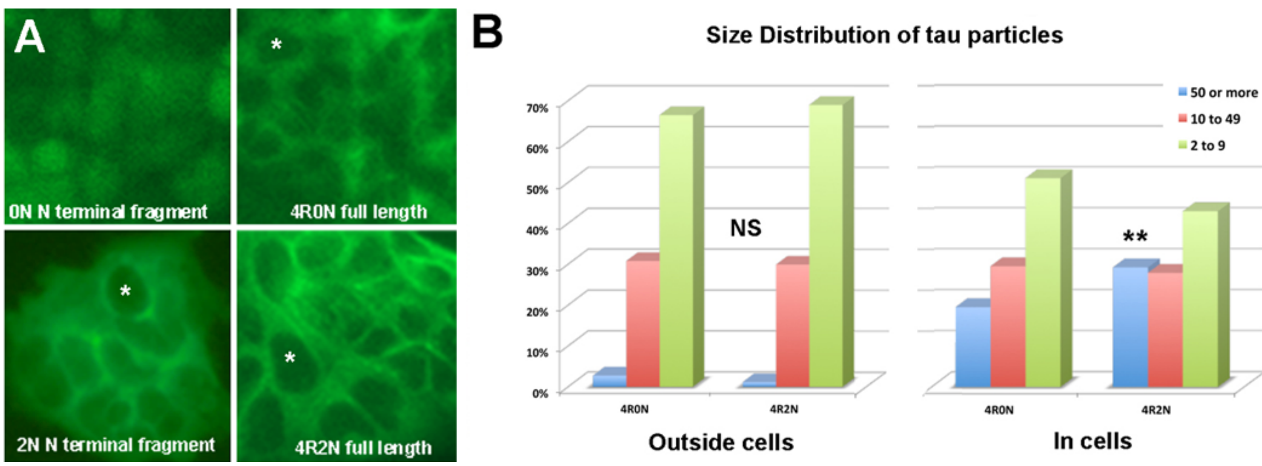

Figure 21 **Tau uptake and nuclear localization by neuroblastoma cells in culture reveals E2/3 isoform correlated patterns** **Panel A:** Full length (4R) and N terminal only (residues 1-255, excluding the MTBR) show E2- specific nuclear uptake of N terminal, but not full length tau species when expressed in P19 neuroblastoma cells. Asterisks show tau-negative nuclear profiles. This pattern suggests that selective tau E2+ uptake seen in very early AD is not modulated by proteolytic liberation of the tau projection domain, which has been a demonstrated consequence of both AD cytopathology and of tau overexpression (Hall et al 2000). **Panel B:** GFP-tagged tau purified from overexpressing bacterial cultures are taken up into differentiated SH-SY5Y cells and washed, fixed and examined after overnight incubation shows that intracellular and extracellular tau particles are readily distinguished from one another by a simple ImageJ size analysis, with relatively large particles (50 or more pixels) being found only in intracellularly located profiles ($p << 0.0001$, Chi square test). There was a more subtle, but still significant size difference between internalized 4R0N and 4R2N tau particles ($p < 0.02$, Chi square test, double asterisk), with 4R2N tau particles predominating in the largest size class.

2B Summary of new data obtained and analyses performed during the NCE

Nuclear localization of tau expressed in P19 cell lines Despite our difficulties in achieving differentiated neuronal phenotypes in neuroblastoma cell lines, we have successfully used G418 selection to isolate stable P19 lines expressing N-terminus E2- tau, N-terminus E2+ tau, full-length (4R) E2- tau, and full-length (4R) E2+ tau. Differentiation of these cells is sufficient to show that the N-terminus tau that lack axon binding domain (4R) showed significantly less localization to processes than to the cell body, whereas the full-length tau showed evenly signal distribution on both processes and cell body (not shown in this report). In light of new IHC data derived from our

new E2+ tau mAb (4G11), we have used the G418 selected lines to develop a nuclear tau localization assay in P19 cells (Figure 21A). We found that nuclear localization in P19 cell lines only occurred with the expression of N-terminus half E2- tau (Figure 21A). This finding suggests that the transient increase in nuclear E2+ tau seen in dentate GCs in very early AD is not due to proteolytic cleavage of the tau projection domain, but to some other mechanism, presumably one associated with isoform-specific localization of expression of tau, such as the miRNA-mediated changes associated with the onset of AD (Lau et al. 2013, Hebert et. al. 2010, Smith et. al. 2011, Hansen et. al. 2016).

Modeling N terminal tau isoform contributions to co-oligomerization and "prionlike" tau spreading– materials generation and preliminary experiments One of the more interesting aspects of the major finding of this project (i.e. that N terminal isoform differences are distinctive features of tau secretion and trans-synaptic tau movement and toxicity in AD) is that it raises critical questions about the role and even the relevance of the now widely accepted idea of "prionoid" tau lesion spreading in AD pathogenesis. At the beginning of this project, we began developing cell culture models of N terminal and E2 +/- specific interactions between transferred and endogenous tau as part of Aim 2B, but much of this work was to have depended on axonal and dendritic features that we failed to generate reliably, and was therefore abandoned in favor of more fruitful alternatives emerging from the highly successful Aims 1A and 1B that were congruent with Aim 2B (an example is the nuclear localization study described above and in Figure 20A). However, despite the recent burst of interest in "prionlike" spreading of tau, very little attention has been paid to the modulatory effects of N terminal exons, presumably because they are distant from the tau MTBR, are not themselves aggregation-prone and have little disease literature devoted to them. We have therefore continued efforts to study the effects of E2 and E3 on the co-oligomerization of endogenously expressed tau with tau that is secreted by PSTs and taken up trans-synaptically in cell culture. In particular, we have generated the necessary plasmids, which are summarized in Table 1.

Table 1 Tau expression and transfection vectors for co-oligomerization experiments We have observed that tau aggregate uptake is an active and ongoing process within differentiated SH5Y and NB2A cells with E coli purified tau-GFP being internalized at various sizes. To further investigate this and determine if isoform specificity was a factor or if a single aggregate could act as a seed and continue growing once internalized, we developed a red/green system for identifying interactions between endocytosed and expressed tau species ranging from non-oligomerizing (N terminal constructs) and severely oligomerizing (3PO) mutant species in the context of both 3 repeat (3R) and 4 repeat (4R) MTBR containing tau species. We have generated both EGFP and "cherry" fusion proteins in both mammalian and E. coli – expressible plasmids to facilitate protein generation for uptake (bacterial) and endogenous expression (mammalian).

Mammalian plasmids	Bacterial plasmids
DNA5 EGFP	pQE EGFP
DNA5 3R0N EGFP	pQE 3R0N EGFP
DNA5 3R2N EGFP	pQE 3R2N EGFP
DNA5 4R0N EGFP	pQE 4R0N EGFP
DNA5 4R2N EGFP	pQE 4R2N EGFP
DNA5 N Terminal E2- EGFP	pQE N Terminal E2- EGFP
DNA5 N Terminal E2+ EGFP	pQE N Terminal E2+ EGFP
DNA5 1PO+ 4R2N EGFP	pQE 1PO+ 4R2N EGFP
DNA5 2PO+ 4R2N EGFP	pQE 2PO+ 4R2N EGFP
DNA5 3PO+ 4R2N EGFP	pQE 3PO+ 4R2N EGFP
DNA5 1PO- 4R0N EGFP	pQE 1PO- 4R0N EGFP
DNA5 2PO- 4R0N EGFP	pQE 2PO- 4R0N EGFP
DNA5 3PO- 4R0N EGFP	pQE 3PO- 4R0N EGFP
3.1 Cherry	pQE Cherry
3.1 3R0N Cherry	pQE 3R0N Cherry
3.1 3R2N Cherry	pQE 3R2N Cherry
3.1 4R0N Cherry	pQE 4R0N Cherry
3.1 4R2N Cherry	pQE 4R2N Cherry
3.1 N Terminal E2- Cherry	pQE N Terminal E2- Cherry
3.1 N Terminal E2+ Cherry	pQE N Terminal E2+ Cherry

These plasmids encode N terminal and full length E2- and E2+ tau species and also mildly (1PO) to severely (3PO) aggregation-prone mutants (Iliev et. al. 2006). A number of these have already been expressed in stable SH-SY5Y and P19 lines (see Figures 21A and 22). We have also begun characterizing uptake and oligomerization using purified EGFP and cherry-tagged tau species, as shown in Figure 22. Key questions to be addressed in the future include: What effect does E2 have on tau uptake, co-aggregation propensity and toxicity? How is soluble or insoluble tau entering the cell? Does aggregation state correlate with toxicity in the same way in E2+, E2-, 3R and 4R specific contexts?

Figure 22 3R0N tau internalization by SH-Sy5Y cells after 24 hours of incubation We have demonstrated reliable aggregation of full length 3R and 4R E2- (0N) tau in vitro and have shown that it is taken up within SH-SY5Y cells After 24 hours of incubation with aggregated 3R0N-GFP Tau and two PBS washes the SH5Y cells show varying levels of internalization, with a majority of cells having at least a single particle. Localization is apparently to non-nuclear endocytic vesicles (according to phase contrast and side-scatter images) and also probably to lysosomes. GFP signal begins decreasing and bluring post uptake, leading us to believe that aggregates are being lysed. After 24 hours of incubation with aggregated 3R0N-GFP Tau and two PBS washes, NucBlue was added for 20 mins. Columns shown are bright field, merged (BR+488), 488, flow cytometry side scatter and NucBlue.

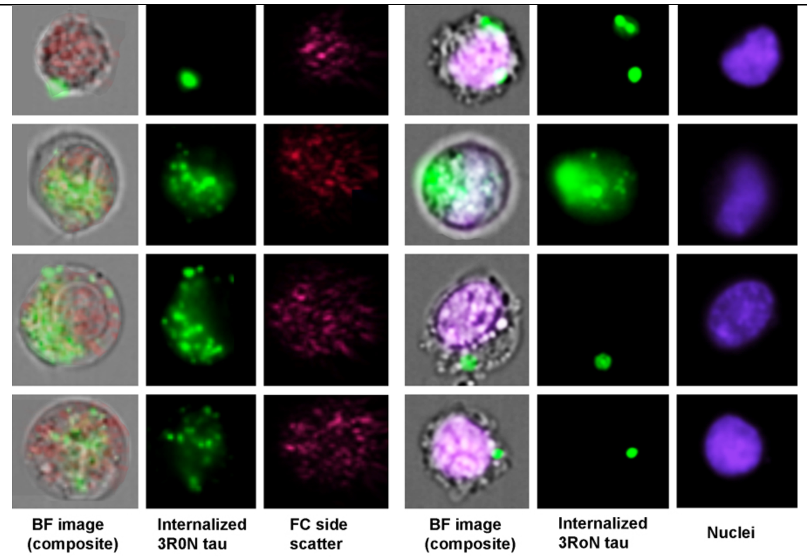

4. Key research accomplishments

1) Identification and characterization of a "fingerprint" set of 47 CSF proteins recruited to exosome-like microvesicles (EMV30-200) in early AD (Braak Stage 4). We define "fingerprint" proteins as being a) identified at high stringency in samples from multiple patients, b) upregulated in early AD and c) known to interact physically with both one another and with Abeta and/or tau in AD pathogenesis. GO term functional analysis of these proteins show them to be involved in functions critically affected in early AD pathogenesis. A significant minority of the proteins in our fingerprint have been identified previously as potential candidate biomarkers for early AD.

- ELISA analysis of the Braak Stage 4 exosomal CSF samples showed **significantly higher proportions of E2-tau isoforms** (i.e. tau species containing the Exon1-Exon 4 junction sequence) than was true of other AD stage samples and of hippocampal homogenate EMV30-200 samples. The potential significance of this for our understanding of AD pathogenesis is highlighted by the results of our IHC study (summarized below).
- A major finding made during the NCE for this project is that **our fingerprint is significantly enriched in targets of neuronal microRNAs, particularly one (miR132-3p) known to regulate tau splicing and to be downregulated in early AD**. This neatly accounts for the remarkable enrichment of fingerprint proteins in gene products that are selectively upregulated in AD, since miRNAs recruited to exosomes have typically inhibitory effects on the localized expression of target genes. It also accounts for the

presence of 2 multipatient proteins that do not interact with tau/Abeta (REST and DICER1) but are known to regulate miR132-3p production and that other AD-selective miRNAs (Lu et. al. 2014, Hebert et. al. 2010).

2) Identification of flocculent E2-tau dominant tau lesions (FTLs) in the dentate and CA1 in AD as new tau lesion types In the DG, E2-tau dominant interstitial deposits in the vicinity of swollen PP terminals within the granule cell dendritic fields are associated with the localized loss of MAP2 immunolabel but not NFT formation within postsynaptic granule cell dendrites. While FTL-like tau deposits in the DG molecular layer have been alluded to in the literature based on phosphotau immunolabel (usually AT8), their flocculent appearance, association with PP terminals, predominantly extracellular nature, apparent toxicity to GCs and E2- isoform specificity have not been and are thus novel, justifying their classification as a "new" tau lesion. The presence of FTLs and almost total absence of NFT-like tau deposits in DG molecular layers indicate that FTLs in the dentate molecular layers are purely due to anterograde tau transport and secretion from axons and axon terminals originating in the EC.

- **FTL lesion formation in both DG and CA1 in AD appears to be correlated with localized A beta accumulation** and thus may be involved in SP formation and toxicity in AD. In the DG, there was a clear tendency for E2-tau immunopositivity to develop before A beta label, since we observed the former frequently in the absence of the latter, especially in early Braak Stage (AD2/AD3) samples. This includes the (toxicity-associated) localized loss of MAP2 immunolabel in postsynaptic dendrites in FTLs. This pattern was not identifiable in CA1 or subiculum, very likely due in part to the much greater lesion diversity of these areas.
- **There was a significant negative correlation between A beta immunolabel intensity and E2- dominance in FTLs in the DG.** E2- tau dominance was strongest where A beta label was either absent or relatively weak. This was true of both interstitial tau deposits and intra-teminal label. This finding is particularly interesting in light of the E2- tau associated toxicity in early FTLs, as it suggests that the A beta associated changes might involve a different (E2+ tau associated) toxicity pathway. Both pathways (pre-A beta, E2- tau and post A beta, E2+ tau) would appear to involved the tau N terminus, since localized 9G3 tau immunolabel (specific for fyn-phosphorylated Y18 in the tau N terminus) was was always present (not shown in this report – reported earlier).

We also identified another E2 isoform specific change correlated with AD progression – **the depletion of nuclear E2+ tau -** in the DC granule cell layer. The significance of this change to AD pathogenesis remains unclear.

3) We found that FTLs resembling those characterized above in AD also developed in later stage (CTE3/CTE4) HC samples. These resembled the FTLs described above in AD samples in their overall size, constituents and properties in the DG molecular layers (plaque-shaped E2-dominant interstitial and intraterminal tau accumulations with toxicity to local GC dendrites) that were typically associated with A beta deposits, as in our AD cases. However, they exhibited 2 potentially important differences from DG FTLs in AD:

- **AMGs (i.e. Iba1-labeled, low circularity, DAPI-positive profiles) were clearly more localized to FTLs** than other loci in DG molecular layer fields in CTE than they were in AD.

- **Significant correlations between E2-/E2+ immunolabel ratios and the intensity of A beta immunolabel that were prominently evident in AD4/5 were not evident in our CTE3/4 samples**, although a nearly significant (p ~ 0.06) correlation was noted between increased relative E2+ label and A beta intensity. This may merely be due to low sample size, the high inherent variability of CTE lesions, or the fact that staging is less well established in CTE than in AD.

These differences are consistent with a more central role for A beta in AD than for CTE, as suggested by other recent studies (McKee et. al. 2013). We also found that CTE3/4 cases exhibited changes in nuclear E2+ localization in dentate GCs similar to but not identical to those seen in AD samples, which also showed a marginally significant increase in nuclear E2+ tau label in 2 of our very early AD samples. As with AD, we are not yet sure what this means.

4) Other results of this project We have begun modeling nuclear localization of E2+ tau in cell culture (P19 cells), and preliminary indications are that proteolytic cleavage of E2+ tau, but not E2- tau, is insufficient to induce increased localization to the nucleus. This may in turn suggest that a) nuclear localization increases are independent of N terminal proteolytic fragment generation in AD and b) that nuclear depletion of E2+ tau in later stages of both AD and CTE is dependent on E2+ specific sequestration via intracellular tau aggregate formation. We have generated tools (EGFP and cherry labeled tau constructs) to test the latter possibility in cell culture.

5. Conclusions and impact

The most important result of this project appears to be the validation of the main idea behind its initial rationale: i.e. that the tau projection (N terminal) domain and the N terminal domain splice variants (E2- and E2+ tau) play critical but poorly studied and poorly understood roles in AD pathogenesis, and that there are links between N terminal tau roles in AD and the role(es) played by tau in the propagation of CTE lesions to the hippocampus. This was completely validated and given more context by the Aim 1 investigations and is at least consistent with E2- tau specific effects from Aim 2. is both completely novel and congruent with some of the most exciting and puzzling recent findings in the field (e.g. the role of miRNAs and the nature of the link between A beta misprocessing and tau-mediated toxicity, respectively). The additional findings that E2- specific tau release from axons and axon terminals a) accounts for much of the interstitial tau at primary CTE lesions and in FTL-like lesions in the DG, b) occurs in advance of or in conjunction with visible A beta deposition and c) is correlated with significantly more activated microglial localization in the latter in CTE than in AD, indicates a clear link between CTE and AD pathogeneses via tau. These results have implications that should have major impacts on AD and CTE research:

- Recently emerging information about secreted exosome and miRNA mediated dysfunction in AD suggests that our observations of highly anomalous AD-specific changes in the CSF exosomal proteome can be accounted for by the decreased production and/or exosomal recruitment of specific microRNA species (e.g. miR 132-3p) known to be downregulated at the onset of AD and to modulate tau splicing and the expression of AD-relevant genes.

- E2- dominant hippocampal tau lesions (FTLs with diffuse plaque-like morphology and swollen PSTs) may be the result of afferent transport and secretion from perforant pathway

terminals, and that mixed or E2+ dominant lesions formation is regulated differently, possibly by a combination of retrogradely transported signals from the EC (NFTs) and/or as a consequence of afferent-derived A beta toxicity via FTLs. We conclude that the E2-dominant FTLs that develop in the DG in CTE differ from those in AD in that neuroinflammatory processes via activated microglia are more important and A beta somewhat less important than in the development of very similar lesions in AD.

Our results also raise larger questions relevant to a major trend in current neurodegenerative disease (NDD) research; i.e. the tendency to ascribe a central and even a driving common role to 'prionlike' lesion spreading mechanisms in most or all NDDs associated with protein aggregate formation. Our results affirm the disease-relevance of the tau projection domain and suggest a strong role for miRNA mediated dysfunction in AD, both of which appear incompatible with "prionoid" hypotheses. These results have caused me (the PI) to devote considerable effort to a critical re-evaluation of prionoid mechanisms of NDD pathogenesis, which is the subject of a MS (currently nearing completion) that a former student of mine and I are now writing (Lum & Hall – see below).

6. Publications, Abstracts and Licenses

Abstract

- Hall, G.F. (2013) Systems-based analysis of proteins recruited to exosomes by 4R0N overexpression and in AD. 2013 Cantoblanco Workshop, Madrid, Spain.

Published MS:

- Gendreau K, Hall GF (2013) Tangles, toxicity, and tau secretion in AD – New approaches to a vexing problem. *Front Neurol* 4, 160.
- Bhatia N and Hall, GF Untangling the role of tau in AD - A unifying hypothesis *Translational Neuroscience* 2013 4(2) 117-133. DOI: 10.2478
- Saman S, Lee N, Inoyo I, Jin J, Li Z, Doyle T, McKee AC, Hall GF (2014) Proteins Recruited to Exosomes by Tau Overexpression Implicate Novel Cellular Mechanisms Linking Tau Secretion with Alzheimer's Disease. J Alz Dis: DOI:10.3233/JAD-132135
- Hall, GF (2014) Report from the Tau Front: Cantoblanco 2013 J Alzheimers Dis Parkinsonism 4, e133

MSs in Preparation/Review

- Hall GF, Jin J, AlBattah R, Nguyen K, Alkaraki A, Viswanathan R, Li Z, Lee N, Alvarez VE, Goldstein L, McKee AC, and Saman S. Changes in the CSF exosomal proteome in early Alzheimer's Disease yield a proteomic "fingerprint" that is correlated with elevated exon 2- tau species
- Nguyen K and Hall GF Biofluids and the Expanding Exoverse: A New Approach to Diagnosis?
- Lum SZ and Hall GF A critical re-evaluation of the "prionoid" hypothesis of neurodegenerative disease
- Patuto B, McKee A, Goswami D, Alvarez VE, Huber R, Jin J and Hall GF. Does tau drive plaque formation in AD and CTE? A comparative study of A beta and the tau projection domain in the biogenesis of senile plaques in Alzheimer's Disease and Chronic Traumatic Encephalopathy

7. Inventions, Patents or Licenses

Patent: **A novel, inexpensive method for the early diagnosis of Alzheimer's disease** Final approval February 15, 2015, US Patent number 61299198

8. Milestone Deliverables

Milestone	Baseline Plan Date	Completion Date
Aim 1A E2+/- sensitivity and specificity Exosome analysis of CSF and brain homogenates	10-31-2014	11-30-2015 (acquisition) 12-31-2016 (analysis)
Aim 1B E2+/- sensitivity and specificity IHC on paraffin embedded brain sections (AD and CTE)	04-15-2014	9-30-2016 AD 6-10-2017 CTE, analysis
Aim 2A Interactions between tau and the Exosomal Proteome Plasmid & cell line construction, proteome analysis	10-31-2014	12-31-2015 (cell lysates) 12-31-2016 (media exosomes)
Aim 2B Interactions between tau and the Exosomal Proteome Characterization of secreted proteins from cultures and tissues (revised due to failure of adequate cell differentiation)	04-15-2015	Initial goals not achieved 4-30-2017 (revised goals – see report for details)

9. Other Achievements:

Degrees Awarded: Raid Al-Battah (Ph.D)
Almuthanna Alkaraki (Ph.D)
Sarvani Manne (MS)

10. References:

Abrahamsen H, Stenmark H. Protein secretion: unconventional exit by exophagy. *Curr Biol* 2011 20, R415-418.

Antonell A, Lladó A, Altirriba J, Botta-Orfila T, Balasa M, Fernández M, Ferrer I, Sánchez-Valle R, Molinuevo JL A preliminary study of the whole-genome expression profile of sporadic and monogenic early-onset Alzheimer's disease. *Neurobiol Aging* 2013 **34**, 1772-1778.

Bhatia N and Hall, GF Untangling the role of tau in AD - A unifying hypothesis *Translational Neuroscience* 2013 4(2) 117-133. DOI: 10.2478

Blalock EM, Buechel HM, Popovic J, Geddes JW, Landfield PW Microarray analyses of laser-captured hippocampus reveal distinct gray and white matter signatures associated with incipient Alzheimer's disease. *J Chem Neuroanat* 2011 **42**, 118e126.

Blalock EM, Geddes JW, Chen KC, Porter NM, Markesbery WR, Landfield PW Incipient Alzheimer's disease Microarray correlation analyses reveal major transcriptional and tumor suppressor responses. *Proc Natl Acad Sci U S A* 2004 **101**, 2173-2178.

Franceschini, A., Szklarczyk, D., Frankild, S., Kuhn, M., Simonovic, M., Roth, A., Lin, J., (...), Jensen, L.J. STRING v9.1: Protein-protein interaction networks, with increased coverage and integration *Nucleic Acids Research*, 2013 **41** (D1): pp. D808-D815. (Dataset Issue)

Gupta, S., Verma, S., Mantri, S., Berman, N.E., Sandhir, R. Targeting microRNAs in prevention andtreatment of neurodegenerative disorders. *Drug Dev Res*. 2015; **76**, 397-418.

Hall GF, Lee VM, Lee G, Yao J. Staging of neurofibrillary degeneration caused by human tau overexpression in a unique cellular model of human tauopathy. *Am. J. Path* 2001; 158:235-46.

Hansen KF, Sakamoto K, Aten S, Snider KH, Loeser J, Hesse AM, et al. Targeted deletion of miR-132/-212 impairs memory and alters the hippocampal transcriptome. *Learn Mem*. 2016; 23:61–71.

Hebert, S.S., Horr, K., Nicola•, L., Bergmans, B., Papadopoulou, A.S., Delacourte, A., De Strooper, B.,2009. MicroRNA regulation of Alzheimer's amyloid precursor protein expression. *Neurobiol Disease*. 33; 422-428.

Hebert SS, Papadopoulou AS, Smith P, Galas MC, Planel E, Silahtaroglu AN, Sergeant N, Buee L, De Strooper B Genetic ablation of Dicer in adult forebrain neurons results in abnormal tau hyperphosphorylation and neurodegeneration. *Hum Mol Genet* 2010, 19(20):3959–3969

Hyman, BT, Van Hoesen GW, Kromer LJ , and Damasio AR, Perforant pathway changes and the memory impairment of Alzheimer's disease, *Annals of Neurology* **20**, no. 4, pp. 472–481, 1986.

Iliev AI, Ganesan S, Bunt G, Wouters FS. Removal of pattern-breaking sequences in microtubule binding repeats produces instantaneous tau aggregation and toxicity. *J Biol Chem* 2006; 281: 37195-37204.

Ittner LM, Ke YD, Delerue F, Bi M, Gladbach A, van Eersel J, et al. Dendritic function of tau mediates amyloid-beta toxicity in Alzheimer's disease mouse models. *Cell* 2010; 142:387-97.

Kim W, Lee S and Hall, GF Secretion of human tau fragments resembling CSF-tau is modulated by the presence of the exon 2 insert. *FEBS Letters* 2010 584: 3085–3088.

King, M.E., Kan, H., Baas, P. W., Erisir, A., Glabe, C., and Bloom G. S. Tau-dependent microtubule disassembly initiated by prefibrillar beta-amyloid. *J. Cell Biol*. 2005 175: 541-546.

Lau P, Bossers K, Janky R, Salta E, Frigerio CS, Barbash S, Rothman R, Sierksma AS, Thathiah A, Greenberg D, Papadopoulou AS, Achsel T, Ayoubi T, Soreq H, Verhaagen J, Swaab DF, Aerts S, De Strooper B. Alteration of the microRNA network during the progression of Alzheimer's disease. *EMBO Mol Med*. 2013 5(10):1613-34.

Li L, et al. Expression of 1N3R-Tau Isoform Inhibits Cell Proliferation by Inducing S Phase Arrest in N2a Cells 2016 *PLOS ONE* | DOI:10.1371/journal.pone.0119865

Llorens-Martín M, Blazquez-Llorca L, Benavides-Piccione R, Rabano A, Hernandez F, Avila J, DeFelipe J. Selective alterations of neurons and circuits related to early memory loss in Alzheimer's disease. *Front Neuroanat*. 2014 8:38. doi: 10.3389/fnana.2014.00038.

Lu T, Aron L, Zullo J, Pan Y, Kim H, Chen Y, Yang T-HH, Kim H-MM, Drake D, Liu XS, et al: REST and stress resistance in ageing and Alzheimer's disease. *Nature* 2014, 507, 448-454.

McKee AC, Stern RA, Nowinski C, Stein T, Alvarez VE, Daneshvar D, Lee H-S, Wotjowitz S, Hall GF, Baugh C, Riley D, Kubilus C, Cormier K, Martin B, Abraham C, Ikesu T, Richard RR, Wolozin B, Budson A, Goldstein LG, Kowall, NE, Cantu RC The Spectrum of Disease in Chronic Traumatic Encephalopathy *Brain*. 2013 doi: 10.1093

Milan MJ Linking deregulation of non-coding RNA to the core pathophysiology of Alzheimer's disease: an integrative review *Progress in Neurobiology* (in press)

Prasad, K.N.,. Oxidative stress and pro-inflammatory cytokines may act as one of the signals for regulating microRNAs expression in Alzheimer's disease. *Mech Aging Dev* 2016 6374, 30291-30293.

Rapoport M, Dawson HN, Binder LI, Vitek MP, Ferreira A. Tau is essential to beta -amyloid-induced neurotoxicity. *Proc Natl Acad Sci U S A* 2002; 99:6364-9

Saman S, Kim W, Raya M, Visnick Y, Miro S, Saman S, Jackson B, McKee AC, Alvarez VE, Lee NC, Hall GF (2012) Exosome-associated tau is secreted in tauopathy models and is selectively phosphorylated in cerebrospinal fluid in early Alzheimer disease. *J Biol Chem* 287, 3842-3849

Saman S, Lee N, Inoyo I, Jin J, Li Z, Doyle T, McKee AC, Hall GF Proteins Recruited to Exosomes by Tau Overexpression Implicate Novel Cellular Mechanisms Linking Tau Secretion with Alzheimer's Disease. *J Alz Dis* 2014 DOI:10.3233/JAD-132135

Smith PY, Delay C, Girard J, Papon MA, Planel E, Sergeant N, Buee L, Hebert SS (2011) MicroRNA-132 loss is associated with tau exon 10 inclusion in progressive supranuclear palsy. *Hum Mol Genet* 20: 4016-4024

Talwar, P., Sinha, J., Grover, S. et al. Dissecting Complex and Multifactorial Nature of Alzheimer's Disease Pathogenesis: a Clinical, Genomic, and Systems Biology Perspective *Mol Neurobiol* (2016) 53: 4833.

Uryu K, Chen XH, Martinez D, et al. Multiple proteins implicated in neurodegenerative diseases accumulate in axons after brain trauma in humans. *Exp Neurol* 2007;208:185–92.